The oncogenic FIP1L1-PDGFRα fusion protein displays skewed signaling properties compared to its wild-type PDGFRα counterpart

Serge Haan, Christelle Bahlawane, Jiali Wang, Petr V Nazarov, Arnaud Muller, René Eulenfeld, Claude Haan, Catherine Rolvering, Laurent Vallar, Venkata P Satagopam, Thomas Sauter & Monique Yvonne Wiesinger

View supplementary material

Submit your article to this journal

Article views: 70

View related articles

View Crossmark data

ORIGINAL RESEARCH

The oncogenic FIP1L1-PDGFRα fusion protein displays skewed signaling properties compared to its wild-type PDGFRα counterpart

Serge Haan,[1] Christelle Bahlawane,[1] Jiali Wang,[1] Petr V Nazarov,[2] Arnaud Muller,[2] René Eulenfeld,[3] Claude Haan,[3] Catherine Rolvering,[3] Laurent Vallar,[2] Venkata P Satagopam,[4] Thomas Sauter,[5,*] and Monique Yvonne Wiesinger[5,*]

[1]Molecular Disease Mechanisms Group; Life Sciences Research Unit; University of Luxembourg; Luxembourg, Luxembourg
[2]Genomics Research Unit; Luxembourg Institute of Health; Luxembourg, Luxembourg
[3]Signal Transduction Group; Life Sciences Research Unit; University of Luxembourg; Luxembourg, Luxembourg
[4]Luxembourg Center for Systems Biomedicine; University of Luxembourg; Esch-sur-Alzette, Luxembourg
[5]Systems Biology Group; Life Sciences Research Unit; University of Luxembourg; Luxembourg, Luxembourg

ABSTRACT. Aberrant activation of oncogenic kinases is frequently observed in human cancers, but the underlying mechanism and resulting effects on global signaling are incompletely understood. Here, we demonstrate that the oncogenic FIP1L1-PDGFRα kinase exhibits a significantly different signaling pattern compared to its PDGFRα wild type counterpart. Interestingly, the activation of primarily membrane-based signal transduction processes (such as PI3-kinase- and MAP-kinase- pathways) is

remarkably shifted toward a prominent activation of STAT factors. This diverging signaling pattern compared to classical PDGF-receptor signaling is partially coupled to the aberrant cytoplasmic localization of the oncogene, since membrane targeting of FIP1L1-PDGFRα restores activation of MAPK- and PI3K-pathways. In stark contrast to the classical cytokine-induced STAT activation process, STAT activation by FIP1L1-PDGFRα does neither require Janus kinase activity nor Src kinase activity. Furthermore, we investigated the mechanism of STAT5 activation via FIP1L1-PDGFRα in more detail and found that STAT5 activation does not involve an SH2-domain-mediated binding mechanism. We thus demonstrate that STAT5 activation occurs via a non-canonical activation mechanism in which STAT5 may be subject to a direct phosphorylation by FIP1L1-PDGFRα.

KEYWORDS. AKT; FIP1L1-PDGFRα; Janus kinase; MAP kinase; Platelet-derived growth factor; SH2-domain; Src kinase; STAT-factor

ABBREVIATIONS. CEL, chronic eosinophilic leukemia; Dox, doxycycline; DUSP, Dual-specificity phosphatase; EGR-1, Early growth response protein 1; ERK, extracellular signal regulated kinase; FDR, false discovery rate; F/PDGFRα, FIP1L1-PDGFRα; FRT, Flp recombinase target; HES, hypereosinophilic syndrome; IRF-1, Interferon regulatory factor 1; PDGF, platelet-derived growth factor; PI3K, phosphatidyl-inositol-3-kinase; PLC, phospholipase C; MAPK, mitogen activated protein kinase; MEN, minimal essential network; OSM, oncostatin M; RRHO, rank-rank hypergeometric overlap; RRSP, rank-rank scatter plot; SDEG, significantly differentially expressed genes; STAT, signal transducer and activator of transcription; RTK, Receptor tyrosine kinase; TKI, Tyrosine kinase inhibitor

INTRODUCTION

FIP1L1-PDGFRα (F/PDGFRα) was identified in patients with chronic eosinophilic leukemia.[1,2] A deletion of approximately 800 kb on 4q12 results in the fusion of *FIP1L1*, a pre-mRNA interacting factor, to the catalytic domain of the class III receptor tyrosine kinase PDGFRα. The in-frame fusion event leads to the generation of a constitutively active kinase. F/PDGFRα lacks the entire extracellular and transmembrane region of PDGFRα, inevitable domains that enable membrane localization of the PDGF-receptor protein. Deletion of the transmembrane domain and juxtamembrane region of PDGFRα impairs the autoinhibitory function of this membrane proximal part, causing the constitutive activation of F/PDGRα.[3]

The full length PDGFRα has been studied in great detail and a multitude of tyrosine residues (720, 754, 762, 768, 988 and 1018) have been identified as autophosphorylation sites[4-7] and recruitment of downstream signaling molecules to these motifs has been experimentally confirmed. Tyrosine residues $Y^{572/574}$ have been described as docking sites for signaling molecules such as Src kinases[8,9] as well as STAT factors in the context of the closely related

PDGFRβ.[10,11] Y^{720} was shown to interact with SHP-2[4] and thereby activates the MAP-kinase cascade. Y^{731} and Y^{742} have been identified as recruitment site for PI3-kinase.[12] Y^{1018} and Y^{988} have been shown to mediate association with PLC-$\gamma1$[5] and cCbl.[13] Finally, Y^{849} an autophosphorylation site in the activation loop, is required for kinase activity.[14,15] To our knowledge, Y^{849} has not been described to recruit downstream signaling molecules.

Interestingly oncogenic fusion proteins do not always mirror the signaling behavior of their full length counterpart. For example, Tel-PDGRβ and PDGFRβ signal differently[16] and Hip-PDGFRβ transforms through different pathways than native PDGFRβ.[17]

Here, we show that F/PDGFRα has a modulated signaling capacity compared to PDGFRα: On one hand, F/PDGFRα has a selective defect for activation of the PI3/Akt-pathway which is localization dependent. Other membrane-associated signaling processes (MAPK/Erk-pathway) can be enhanced by forced membrane association. On the other hand, F/PDGFRα potently phosphorylates the STAT factors STAT1, STAT3 and STAT5 via a non-canonical mechanism as it does not require Janus kinase activity.

RESULTS

PDGFRα Wild Type (PDGFRα-wt) and Oncogenic FIP1L1-PDGFRα (F/PDGFRα) Have Different Signaling Patterns

In this study, we aimed at comparing the signaling capacities and transcriptional responses of oncogenic F/PDGFRα with those of the wild type PDGFα-receptor. Activation of the PDGFRα kinase domain leads to activation of various downstream signaling molecules such as phosphatidylinositol (PI3) kinase, PLCγ and Ras/mitogene-activated protein kinase (MAPK) pathways. Hence, we addressed the question whether F/PDGFRα just represents a constitutively active form of the wild type PDGFRα or whether the chimeric F/PDGFRα kinase has different signaling properties.

As overexpression of receptor tyrosine kinases in conventional expression systems generally leads to ligand-independent auto-activation,[18] we used a cellular system which has been successfully used to study the behavior of oncogenic tyrosine kinases.[19,20] This cellular system is based on the site-specific integration of genes of interest at a defined genomic locus (Flp recombinase target site, FRT) and reduces the risk of generating artifacts due to stochastic transgene incorporation. Stable isogenic transfectants were generated by insertion of cDNAs (encoding PDGFRα-wt, F/PDGFRα or related mutants) into the FRT-site in the parental host

cell line. Protein expression is under control of a tetracycline-inducible hybrid CMV/TetO2 promoter and is thus initiated by the addition of doxycycline (Dox). This facilitates the comparison of the signaling capacity of different proteins on a genetically identical background and circumvents cellular alterations which can emerge due to constitutive expression of oncogenic kinases. We have previously used the 293-FR system to investigate the signaling behavior of PDGFRα mutant proteins found in gastrointestinal stromal tumors (GIST). We also showed that the 293-FR-PDGFRα-wt cells reproduce the signaling characteristics of the wild-type PDGFRα if compared to fibroblasts with endogenous expression of wild type PDGFRα.[20]

Induction of protein expression with doxycycline (Dox) was generally performed for 14–18h in order to allow receptor levels to stabilize. Stimulations of the wild type receptor with PDGF-AA were usually performed for 14–18h (in parallel to doxycycline induction) in order to facilitate the comparison of the wild type signals with those of the constitutively active mutants. Stimulation with PDGF-AA for 1h was additionally included for the wild type protein to monitor putative transient signaling events.

For comparison purposes, we included an additional oncogenic mutant of the PDGFRα. This mutant, PDGFRα-D[842]V, is found in patients with gastrointestinal stromal tumors (GIST) and contains a single activating point mutation.[21] We use this mutant protein as a

FIGURE 1. (*See next page*). Wild type PDGFRα and oncogenic F/PDGFRα have different signaling patterns. (**A**) Stable isogenic FRT-cell lines, inducibly expressing PDGFRα or F/PDGFRα were treated with 5 ng/ml doxycycline (Dox) for 18 h. For induction of ligand-induced tyrosine kinase activity, PDGFRα-wild type cells were stimulated with PDGF-AA for the indicated time points. Cellular lysates were analyzed by immunoblotting and stained with phospho-specific antibodies for pPDGFRα, pAKT and pERK1/2. After stripping, the respective membranes were re-probed with polyclonal sera against PDGFRα, AKT and ERK1/2. Finally, blots were counterstained for tubulin (one representative is displayed) to confirm equal loading of the samples. One representative experiment of at least 5 biological replicates is shown. (**B**) Real-time PCR analysis showing the mRNA expression levels of PDGFRα-wt and F/PDGFRα. mRNA was isolated from the corresponding FRT cell lines after treatment with doxycycline for 14h. PDGFRα expression levels are given as normalized relative quantity (NRQ) to the reference genes. A two-way ANOVA with Sidak's test for multiple comparison was used to assess statistical significance (ns: not significant; number of experiments: PDGFRα WT: n = 7; PDGFRα WT (1 h PDGFAA): n = 3; PDGFRα WT (14 h PDGFAA): n = 7; F/PDGFRα (n = 3). Statistical significance was set to 0.05.

control, since it represents another oncogenic PDGFRα mutant, which still contains all domains, including the extracellular and transmembrane region of PDGFRα, in contrast to F/PDGFRα.

First we assessed the stimulation kinetics of the wild type receptor. **Figure 1A** shows that

our experimental system enables the control of RTK activation: Expression of the PDGFRα *per se* does not activate any downstream signaling (**Fig. 1A**, lanes 1 and 2) and stimulation with PDGFAA leads to the activation of downstream molecules (lanes 3–6). As expected PDGFRα wild type is a strong inducer of AKT

FIGURE 1. (*See previous page*).
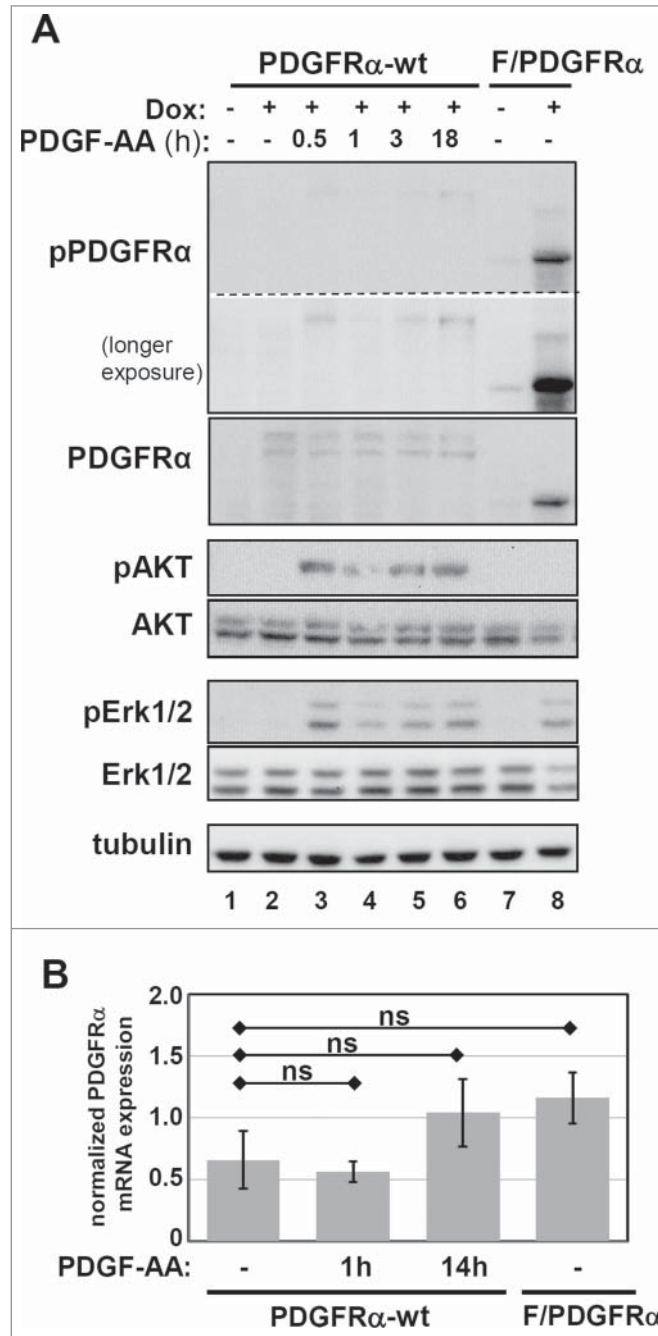
and ERK phosphorylation and the signal persists for longer periods (up to 18h investigated). Unlike PDGFRα wild type, F/PDGFRα completely fails to activate AKT (lane 8) under comparable conditions. Both the wild type receptor and F/PDGFRα activate ERK1/2. It must be noted that activation of the wild-type receptor leads to a much weaker phosphorylation of the receptor (lanes 3–6 vs 8), even at saturating concentrations of PDGF-AA as used here. In addition, we observe higher protein levels for F/PDGFRα compared to the wild-type PDGFRα (see also **Fig. 2C**). We therefore quantified the expression levels of PDGFRα-mRNA in the PDGFRα-wt and F/PDGFRα cell lines. **Figure 1B** shows that the mRNA levels are comparable in both cell lines and do not reflect the observed differences in protein expression. This suggests that the increased protein levels and hyperphosphorylation of F/PDGFRα (and also PDGFRα-D^{842}V, see **Fig. 2C**) are part of the oncogenic phenotype of these mutant proteins.

AKT Activation is Highly Dependent on Spatial Localization of F/PDGFRα

Since the oncogenic signaling pattern induced by F/PDGFRα differs from "conventional" PDGFRα-signaling, we further

investigated the causes for this striking difference. The cytoplasmic localization of F/PDGFRα[22] could offer an explanation for the differences in signaling compared to the integral membrane proteins, i.e. the wild-type PDGFRα receptor and the oncogenic PDGFRα-D^{842}V mutant. Thus, we additionally generated a membrane-attached form of F/PDGFRα (MEM-F/PDGFRα) (**Fig. 2A**). Membrane targeting capacity of the MEM-tag was verified by comparing the localization of MEM-tagged with non-tagged GFP protein using confocal microscopy (**Fig. 2B**).

We then monitored the signaling capacities of MEM-F/PDGFRα and compared them with those of the F/PDGFRα, PDGFRα-wt and the PDGFRα-D^{842}V mutant (**Fig. 2C**). We demonstrate that F/PDGFRα cannot exploit the maximal signaling capacity of the constitutively active PDGFRα-kinase-domain. If compared to PDGFRα-D^{842}V (**Fig. 2C**, lane 1) or the membrane-targeted MEM-F/PDGFRα (lane 6), F/PDGFRα (lane 5) shows absent AKT and strongly reduced MAPK (ERK1/2 and p38) activation. In fact we cannot detect a clear activation of p38 via F/PDGFRα or the wild type PDGFRα protein at these time points (lane 5; lanes 2 to 4), but membrane-association of MEM-F/PDGFRα can augment p38 activation. Membrane localization of F/PDGFRα thus seems to be crucial for inducing the PI3-kinase/

FIGURE 2. (*See next page*). Signaling characteristics of F/PDGFRα. (**A**) Schematic representation of the PDGFRα derived mutant proteins. Δ(F/PDGFRα): Region of PDGFRα deleted in the F/PDGFRα fusion protein. It thus misses the extracellular and transmembrane domains as well as the amino acids 549–578 which contain the Src kinase and potential STAT5 recruitment site; ECD: extracellular domain, TM: Transmembrane region, KD: kinase domain, MEM: membrane targeting tag. (**B**) Membrane recruitment mediated via the generated MEM-tag. MEM-GFP and GFP were stable expressed in 293FR cells and their localization was monitored using live cell confocal microscopy. (**C**) Influence of cellular localization of PDGFRα-proteins on "conventional" PDGFRα signaling. Expression of the *gene of interest* was induced with 5ng/ml doxycycline for 14 h. PDGFRα cells were stimulated with PDGF-AA for the indicated times. Activation of PDGFRα, PLCγ, AKT, ERK1/2 and p38 was assessed by Western blot analysis. One representative experiment of at least 3 biological replicates is shown. (**D**) Ubiquitination of PDGFRα-wt and mutant proteins. The stable cell lines were co-transfected with an HA-ubiquitin expression plasmid and the expression of the PDGFRα, F/PDGFRα and MEM-F/PDGFRα was induced under serum reduced conditions (1% FBS) for 14 hours. Proteasome inhibitor MG132 (10 mM) was added 2 h prior to lysis and PDGF-AA stimulation was performed 1 h prior to lysis. The PDGFRα-wt and mutant proteins were precipitated from the cell lysates using an anti-PDGFRα antibody. HA-ubiquitin and PDGFRα were detected by western blot analysis. One representative experiment of 3 biological replicates is shown.

AKT-pathway activation. Our data clearly show that the cytoplasmic localization of F/PDGFRα impairs AKT activation and does in addition not allow F/PDGFRα to fully exploit its capacity concerning MAPK activation. However, we find that activation of PLCγ is not altered by forced membrane localization of F/PDGFRα. In addition, F/PDGFRα shows a

more prominent activation of PLCγ compared to the stimulated wild type receptor (lanes 3, 4 and 5). Notably, the differences in signaling via the wild-type PDGFRα cannot be explained by the observation of lower protein levels as PDGFRα-wt is able to activate the AKT pathway to a level which is comparable to PDGFRα-D^{842}V and MEM-PDGFRα (lanes 3

FIGURE 2. (*See previous page*).
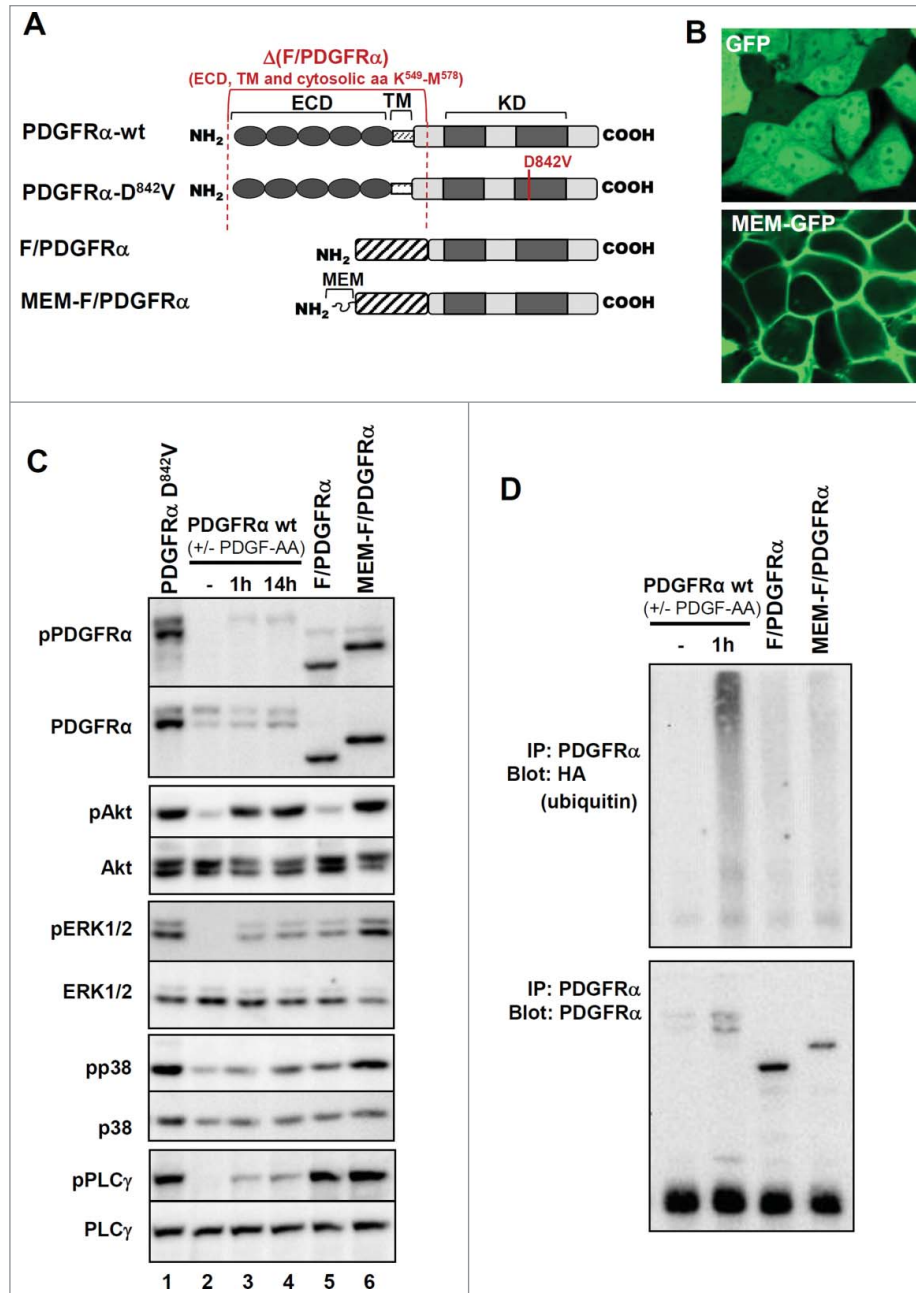
and 4 vs 1 and 6), whereas AKT activation is reduced to cellular background levels in F/PDGFRα cells (lane 2 vs 5).

Reduced Ubiquitination of F/PDGFRα is not Caused by Cytoplasmic Localization

In contrast to PDGFRα-wt the F/PDGFRα fusion protein has been reported to escape ubiquitination.[23] As we observed increased protein levels of F/PDGFRα- compared to PDGFRα-wt, (although mRNA levels were comparable), we were interested in mechanisms that could contribute to the observed differences in protein levels. Since down-regulation of active receptors could be of therapeutic interest, we further investigated if the reduced ubiquitination of F/PDGFRα could be a result of the altered protein localization. Therefore HA-ubiquitin was co-expressed with PDGFRα or F/PDGFRα and ubiquitination of the PDGFRα proteins was assessed. **Figure 2D** shows that PDGF-AA stimulation induces poly-ubiquitination of wild type PDGFRα. On the other hand, both F/PDGFRα and MEM-F/PDGFRα showed reduced ubiquitination. We can thus confirm that ubiquitination of F/PDGFRα is reduced but we additionally show that mere membrane localization is not sufficient to restore poly-ubiquitination as observed for activated PDGFRα wild type. The reduced ubiquitination of F/PDGFRα may thus at least partially contribute to the increased protein levels compared to wild-type PDGFRα.

Activation of STAT Factors is a Hallmark of Oncogenic PDGFRα-Mutant Signaling and Induces Nuclear Translocation and DNA Binding of STAT1, STAT3 and STAT5

RTKs such as PDGFRβ and PDGFRα have previously been described to induce the activation of STATs.[10,240-26] We thus compared the capacity of different PDGFRα proteins to activate STAT transcription factors. Most interestingly we found that only the oncogenic mutants were capable of inducing a strong and prolonged activation of STAT1, STAT3 and STAT5 (**Fig. 3A**). In contrast, neither long- nor short-term PDGF-AA stimulation of PDGFRα-wt induced significant STAT activation in the same setting, although strong activation of AKT and ERK1/2 could be observed at the same time (**Figs. 2C** vs **3A**). In order to confirm our observation that the wild-type PDGFRα is *per se* a very poor inducer of STAT phosphorylation, we stimulated primary human fibroblasts with PDGF-AA and monitored STAT activation in comparison to cells stimulated with the IL-6-type cytokine OncostatinM (**Fig. 3B**). As expected, OSM induced a strong phosphorylation of STAT1, STAT3 and STAT5. In comparison, the wild-type PDGFRs stimulated with PDGF-AA did not lead to a significant activation of STAT factors. We previously showed that if at all detectable, this STAT activation by PDGFRα is weak and very transient.[20] In addition, PDGF-AA stimulation only led to a very transient and weak activation of p38. These findings confirm the signaling pattern observed in our model cell line.

Next we studied whether the constitutively phosphorylated STATs concomitantly translocate to the nucleus and are capable to bind DNA. Therefore we prepared nuclear extracts from cells expressing F/PDGFRα, PDGFRα-$D^{842}V$ or PDGFRα-wt cells stimulated with PDGF-AA for the indicated time periods. First, we performed an electrophoretic mobility shift assay (EMSA) to investigate the binding of STAT5 to an oligonucleotide whose sequence was derived from the β-casein promoter (**Fig. 3C**). By super-shifting the STAT5-DNA-complex using a STAT5 antibody, we confirmed the specificity of the obtained signal. Our results show that DNA binding competent STAT5 translocates to the nucleus in cells expressing oncogenic PDGFRα mutants. We then performed a similar experiment in order to investigate DNA binding of STAT1 and STAT3 (**Fig. 3D**). DNA binding was investigated using an SIE oligonucleotide which allows the detection of STAT1/1 and STAT3/3 homodimeric- as well as STAT1/3 heterodimeric-DNA complexes. As a control, we used Oncostatin M (OSM)-stimulated HepG2 cells showing the formation of the homo- and

FIGURE 3. Unconventional signaling initiated via oncogenic F/PDGFRα. (**A**) Stable 293FR-PDGFRα-wt and -mutant cell lines were treated with doxycycline for 14 h and PDGFRα wild type cells were additionally treated with PDGF-AA for the indicated times. Activation and expression of STAT1, STAT3 and STAT5 was assessed by Western blot analysis. One representative experiment of at least 3 biological replicates is shown. (**B**) Primary NHDF cells were treated with the indicated concentrations of PDGF-AA and OSM for the indicated times and phosphorylation of PDGFR, STAT1, STAT3, STAT5, AKT, ERK1/2 and p38 was monitored by Western blot analysis. A representative tubulin staining was added, showing comparable protein amounts in the samples. One representative experiment of at least 3 biological replicates is shown. (**C**) 293-FR-PDGFRα stable cell lines were treated as described for (**A**). Nuclear extracts were prepared and the formation of STAT5-DNA complexes was analyzed by Electrophoretic Mobility Shift Assay (EMSA) using a β-casein oligonucleotide. The identity of the STAT5/DNA complex was verified by super-shifting the STAT5 band using a STAT5 antibody. One representative experiment of 3 biological replicates is shown. (**D**) 293-FR-PDGFRα stable cell lines were treated as described for (**B**) and the formation of STAT1/STAT1-, STAT1/STAT3- and STAT3/STAT3-DNA complexes was analyzed by EMSA using an SIE oligonucleotide. As a control for the formation of the different STAT1 and STAT3 complexes HepG2 cells were treated with Oncostatin M and analyzed on the same gel. One representative experiment of 3 biological replicates is shown.
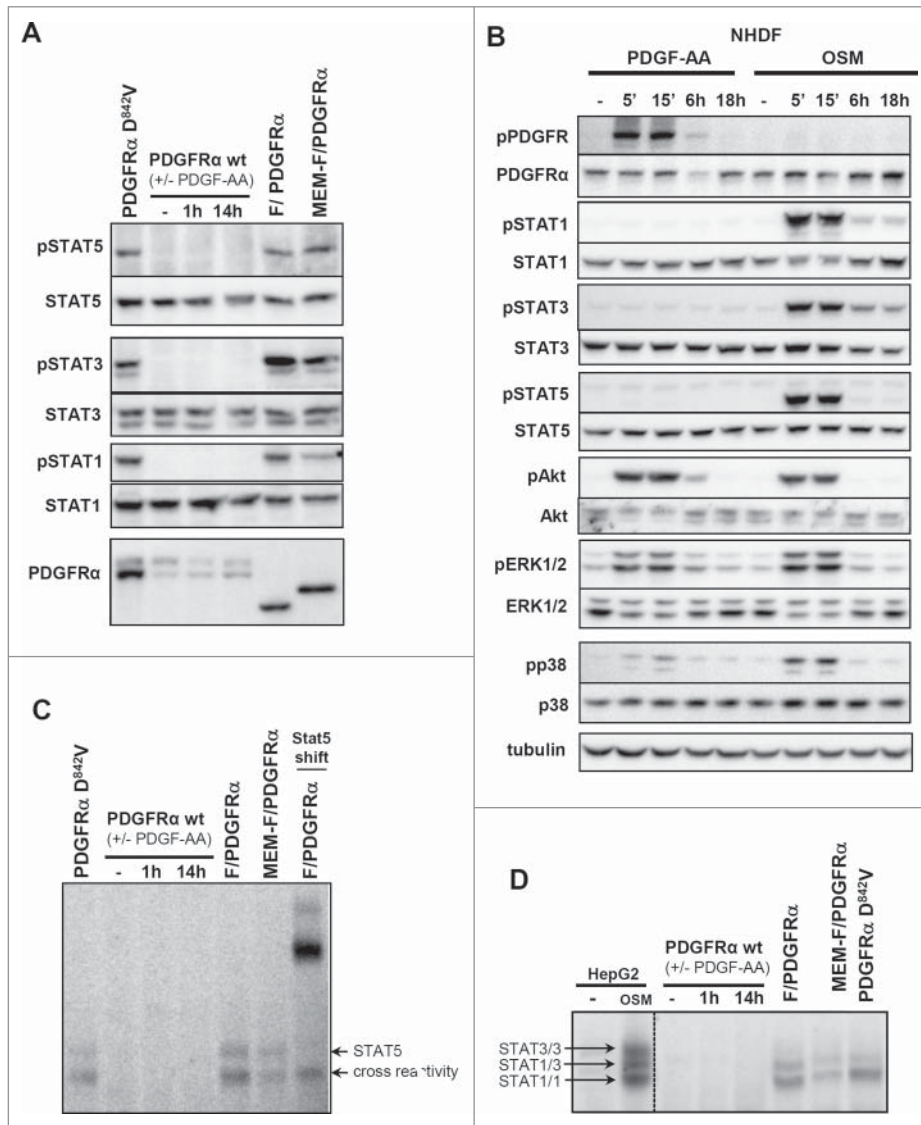
FIGURE 4. STAT phosphorylation by F/PDGFRα does neither depend on Janus kinase nor Src kinase activity. (**A**) Janus kinase activity is not required for F/PDGFRα-mediated STAT5 activation. 293FR-cell lines either stably expressing F/PDGFRα or lacking the persistently activated protein (parental cells) were treated with doxycycline (5ng/ml) for 8h. Simultaneously, the pan-JAK inhibitors JAK inhibitor I (JI-I) or INCB-018424/Jakafi® (INCB; 1 μM) were administered to prevent Jak activation. As a control for Janus-kinase mediated STAT-activation, the parental 293FR-cells were pretreated with inhibitors for 8h and additionally stimulated with OSM (25 ng/ml) for 30 min. Activation of pSTAT1, pSTAT3 and pSTAT5 was assessed by Western blot analysis. One representative experiment of at least 3 biological replicates is shown. (**B**) STAT activation by oncogenic PDGFRa proteins does not require Src kinase activity. MEF cells lacking the Src family kinases Yes and Fyn (SRC++ cells) or lacking Src, Yes and Fyn (SYF cells) were transfected with empty vector (mock) or expression plasmids encoding for F/PDGFRα or PDGFRα-D842V. After 48 h, phosphorylation of STAT1, 3 and 5 was monitored by Western blot analysis. A representative tubulin staining is added, showing comparable protein amounts in the samples. One representative experiment of 3 biological replicates is shown.

heterodimers of STAT1 and STAT3. Again, we found that only the oncogenic PDGFRα-mutants were able to induce DNA binding of STAT1 and STAT3. We found the STAT1/1 and STAT1/3 species to be predominantly formed whereas the STAT3/3 complex was hardly detectable. This indicates that the phosphorylated STAT3 is primarily included in STAT1/STAT3 heterodimers. In addition, the comparison with OncostatinM (OSM)-induced STAT activation shows that the extent of STAT activation via F/PDGFRα is comparable to cytokine-induced signals (**Fig. 4A**, lanes 2 vs. 6). We could thus demonstrate that the phosphorylation of all 3 STAT factors leads to their nuclear translocation. This clearly suggests that STAT factors contribute to the expression of a modified transcriptional
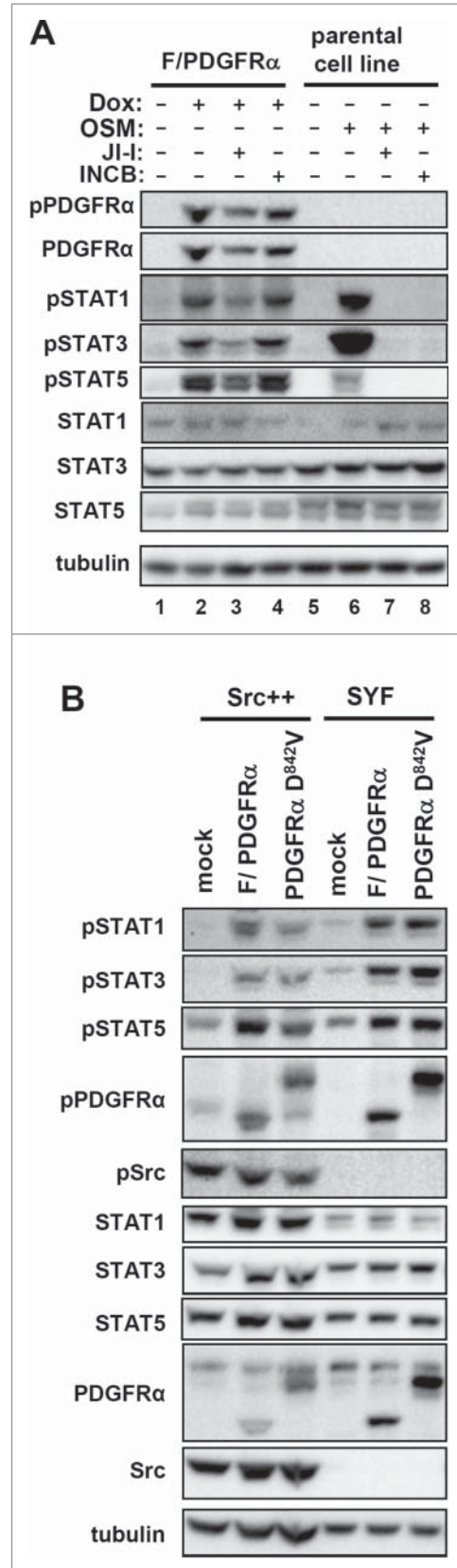
network compared to conventional PDGFRα-wt signaling.

STAT Activation via F/PDGFRα is Independent of Janus Kinases (Jak) and Src Kinases

With regard to developing alternative therapeutic strategies it is paramount to investigate the molecular mechanisms that govern STAT activation via F/PDGFRα. Identifying or excluding the contribution of upstream mediators is crucial as it is known that the activation mechanism of STAT factors by oncogenic kinases can significantly differ. Canonical STAT activation occurs via the activation of upstream Janus kinases. In part, Janus kinase activation has also been implicated in RTK-dependent activation of STAT factors. However, the reports concerning the involvement of Jaks in RTK signaling are conflicting[27,28] and thus we wanted to assess whether Jak-activation is required for F/PDGFRα-mediated STAT activation. We selected 2 different pan-JAK-inhibitors that are effective in the nano-molar range: Jak Inhibitor I (JI-I) and Jakafi[TM]/Ruxolitinib (INCB018424). The latter inhibits JAK1, JAK2 and JAK3 with IC50 of 2.7 nM, 4.5 nM and 322 nM (values determined by *in vitro* kinase assays) respectively and received FDA approval for the treatment of myelofibrosis.

We treated F/PDGFRα-expressing cells with both inhibitors and monitored downstream activation of STAT1, STAT3 and STAT5 (**Fig. 4A**). In order to avoid potential cooperative effects between Jaks and F/PDGFRα at the onset of signaling, we administered the TKIs in parallel to the induction of F/PDGFRα expression. As a control for Jak-mediated STAT activation, we stimulated the parental cell line 293FR with OSM in the presence or absence of the inhibitors (lanes 6 to 8). We show that OSM-mediated STAT activation is totally abrogated in the presence of both inhibitors (lanes 7,8). In stark contrast, treatment of F/PDGFRα cells with Jak Inhibitor-I (JI-I) or INCB-018424 (INCB) did not disrupt constitutive STAT1, STAT3 and STAT5 activation in these cells (lanes 3,4). This demonstrates that

Jak activation is not required for F/PDGFRα-mediated STAT activation.

As Src kinases have also been reported to be involved in the oncogenic activation of STAT factors,[29,30] we investigated whether these kinases could be involved in STAT activation via mutant PDGFRα proteins. For this, we expressed both F/PDGFRα and the GIST mutant PDGFRα-D[842]V in MEF cells expressing the Src kinase (Src++ cells, Yes and Fyn deficient) or lacking expression of all Src kinases (SYF cells, Yes, Fyn and Src deficient). **Figure 4B** shows that both PDGFRα mutant proteins induce the phosphorylation of STAT1, STAT3 and STAT5 in both of these fibroblast cell lines, demonstrating that STAT activation via these mutant proteins does not depend on Src kinases.

Activation of STAT5 Does Not Require an SH2-Mediated Recruitment of STAT5 to Receptor Phosphotyrosine Motifs

Due to the reported importance of STAT5 for myeloid transformation,[31-33] we focused the mechanism of STAT5 activation via F/PDGFRα in more detail. Tyrosine-based recruitment mechanisms are the classical activation mechanisms for STAT factors. Several reports described that the sequence containing Y^{579}/Y^{581} of PDGFRβ constitutes a STAT-binding motif.[10,11] Due to the high sequence and functional homologies between the PDGFRβ and PDGFRα, this motif (Y^{572}/Y^{574}) is regarded to be a potential STAT5 recruitment site in the context of PDGFRα. Interestingly, this described recruitment site is located in the juxtamembrane region of the PDGFRα-wt and is missing in the F/PDGFRα fusion protein, although STAT5 phosphorylation was reported.[1,34] To study the details of STAT5 activation, we therefore generated a series of tyrosine to phenylalanine mutations in our oncogenic PDGFRα proteins (**Fig. 5A**). In order to verify whether the double tyrosine motif Y^{572}/Y^{574} could be involved in the activation of the GIST mutant PDGFRα-D[842]V, we generated a stable cell line expressing a tyrosine to phenylalanine mutant of this protein

(**Fig. 5A**). **Figure 5B** (last lane) shows that STAT5 activation via PDGFRα-D^{842}V does, like F/PDGFRα, also not require the Y^{572}/Y^{574} motif. This result further supports our finding that Src kinases are not involved in activation as this motif is also the reported recruitment site for Src kinases.[35]

A recent report by Noël et al. indicated that tyrosine Y^{720} in F/PDGFRα mediates ERK1/2 activation and is additionally involved in STAT5 activation.[36] We thus generated a F/PDGFRα-Y^{720}F mutant in order to assess STAT5 activation via this mutant protein. As shown in **Figure 5C**, we can confirm the reported requirement of Y^{720} for ERK1/2 activation. However, phosphorylation of STAT5 is not affected by the Y^{720}F mutation, showing that this tyrosine is not absolutely required for STAT5 activation via F/PDGFRα. Similarly, the Y^{720}F mutation within PDGFRα-D^{842}V does not affect STAT5 activation (data not shown).

We decided to analyze the remaining tyrosine motifs within the F/PDGFRα protein in regard to their capability to recruit STAT factors. For this, we generated 2 types of mutant proteins. First, we constructed a deletion mutant (1–29-F/PDGFRα, **Fig. 5A**) in order to test whether the FIP1L1 moiety is involved in STAT5 activation. This mutant only encompasses the first 29aa of the FIP1L1 sequence and therefore lacks 7 tyrosines that could serve as potential recruitment sites. Furthermore, we analyzed which tyrosine motifs within the PDGFRα moiety might serve as recruitment sites for STAT5 in order to mutate potential STAT5 recruiting tyrosines to phenylalanine. The PDGFRα moiety of F/PDGFRα contains a total of 26 tyrosine residues, 12 of which are located in the flexible juxtamembrane, kinase insert and C-terminal region of the receptor (**Fig. 6A**). Further 14 tyrosine residues are located within the kinase domain including the activation loop tyrosine Y^{849} which is a known

FIGURE 5. (*See next page*). STAT phosphorylation by F/PDGFRα does neither depend on Janus kinase nor SH2-domain. (**A**) Schematic representation of the tyrosine to phenylalanine mutations and the deletion mutation generated for F/PDGFRα and PDGFRα-D^{842}V. (**B**) The tyrosine motif Y^{572}/Y^{574} is not required for STAT5 activation via the oncogenic PDGFRα proteins. Expression of the different PDGFRα proteins was induced with 5ng/ml doxycycline for 18 h and stimulation with PDGF-AA performed where indicated. Activation of PDGFRα, STAT5 and AKT was assessed by Western blot analysis. A tubulin staining was performed to monitor the loading of the samples. One representative experiment of at least 5 biological replicates is shown. (**C**) Mutation of Y^{720} does not affect STAT5 phosphorylation. Expression of PDGFRα-wt, F/PDGFRα and F/PDGFRα-Y^{720}F was induced by 5 ng/ml doxycycline for 18 h where indicated. PDGFRα-wt was additionally stimulated with PDGF-AA for 18 h. Activation of STAT5 and ERK1/2 was assessed by Western blot analysis. A tubulin staining was performed to ensure equal loading of the samples. One representative experiment of at least 5 biological replicates is shown. (**D**) Tyrosine-based recruitment motifs within F/PDGFRα are not required for STAT5 activation. Expression of F/PDGFRα, F/PDGFRα-F12 and (1–29)-F/PDGFRα was induced by 5 ng/ml doxycycline for 18 h where indicated. Activation of PDGFRα and STAT5 was assessed by Western blot analysis. A tubulin staining was performed to control for equal loading of the samples. One representative experiment of at least 3 biological replicates is shown. (**E**) A functional STAT5 SH2 domain is not required for F/PDGFRα-mediated STAT5 activation. FRT-cell lines, either stably expressing F/PDGFRα or lacking the persistently activated protein (parental cells), where additionally stably transfected with a construct encoding GFP-tagged STAT5 or GFP-tagged STAT5R^{618}Q-mutant, for which the SH2 domain has been knocked-out. F/PDGFRα expression was induced by doxycycline induction (5 ng/ml) for 18 h where indicated. As a control for the knockout of phosphotyrosine-dependent and SH2 domain-mediated STAT5 recruitment, the parental cells were stimulated with 25 ng/ml OSM for 30 min. Activation of PDGFRα and STAT5 was assessed by Western blot analysis. A tubulin staining was performed to control for equal loading of the samples. One representative experiment of at least 3 biological replicates is shown.
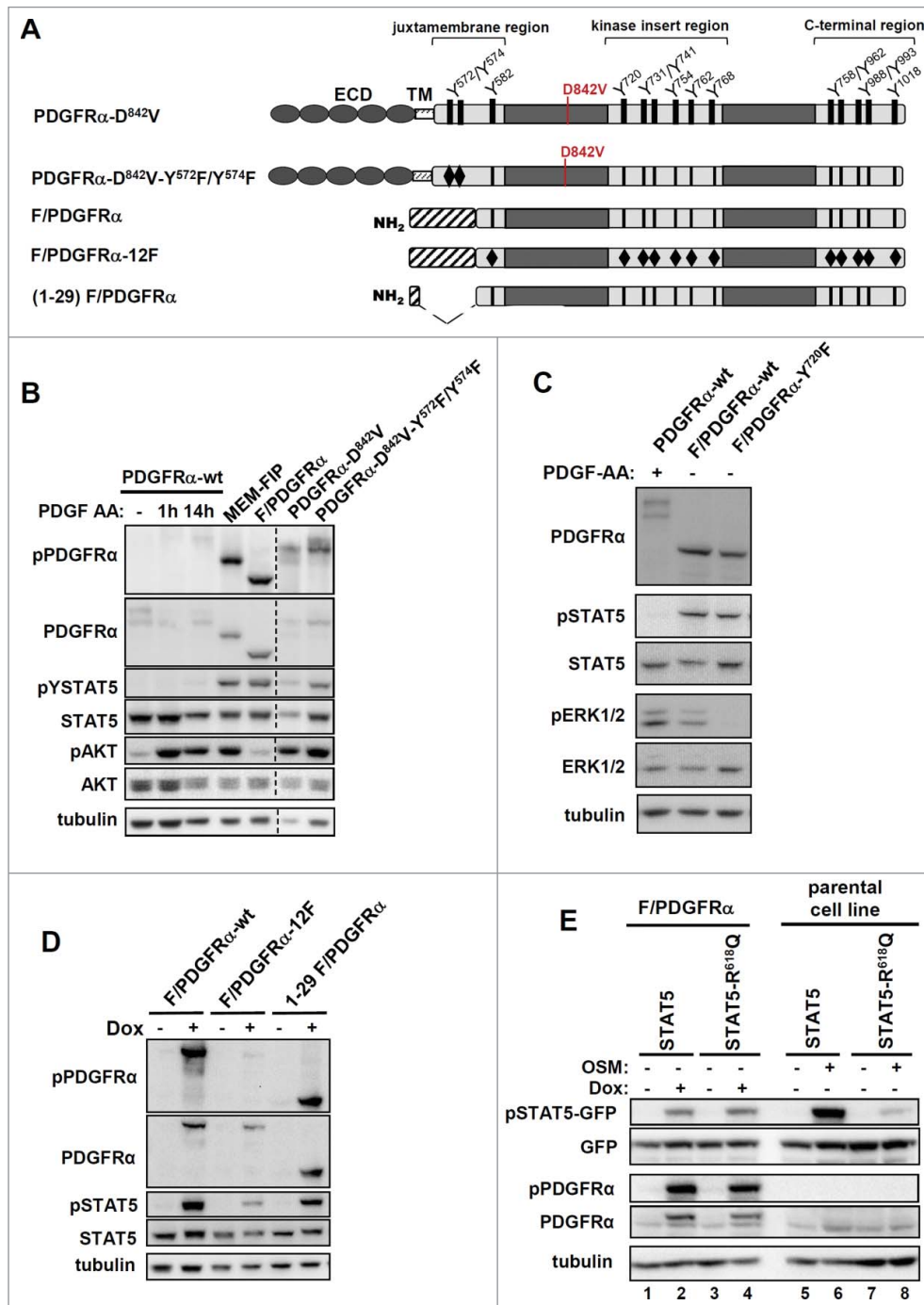
FIGURE 6. Modeling-guided mutagenesis of the F/PDGFRα protein. (**A**) Alignment of the amino acid sequences of human PDGFRα and c-Kit. Conserved residues are indicated in red. The start of the PDGFRα sequence present in the F/PDGFRα fusion protein is indicated by a green arrow. The core of the kinase domain structure is highlighted by a green box and the secondary structure of the Kit template structure used for modeling is indicated (h: helix, s: β strand). The variable kinase insert region is indicated by a yellow box. Buried PDGFRα residues in the kinase domain core structure with a relative solvent accessibility below 20% or 30% are highlighted in dark gray and light gray, respectively. The numbering of the tyrosine residues is given above the sequence. For the core region of the kinase structure, the relative solvent accessibility (in %) of tyrosines is given after the number. Tyrosine residues in the core region of the kinase (and corresponding residues in the Kit structure) which are involved in structural contacts (based on the Kit structure) are underlined. Residues mutated in this study are highlighted in yellow. (**B**) Representation of the solvent accessible surface of the generated PDGFRα kinase domain model (corresponding to amino acids Q^{579} to P^{955} of the F/PDGFRα protein). The core of the kinase domain is colored in green, the kinase insert region is represented in yellow and the activation loop of the kinase is highlighted in pale yellow. Tyrosine residues within the kinase core structure are colored in blue (carbon atoms) and red (oxygen atom).
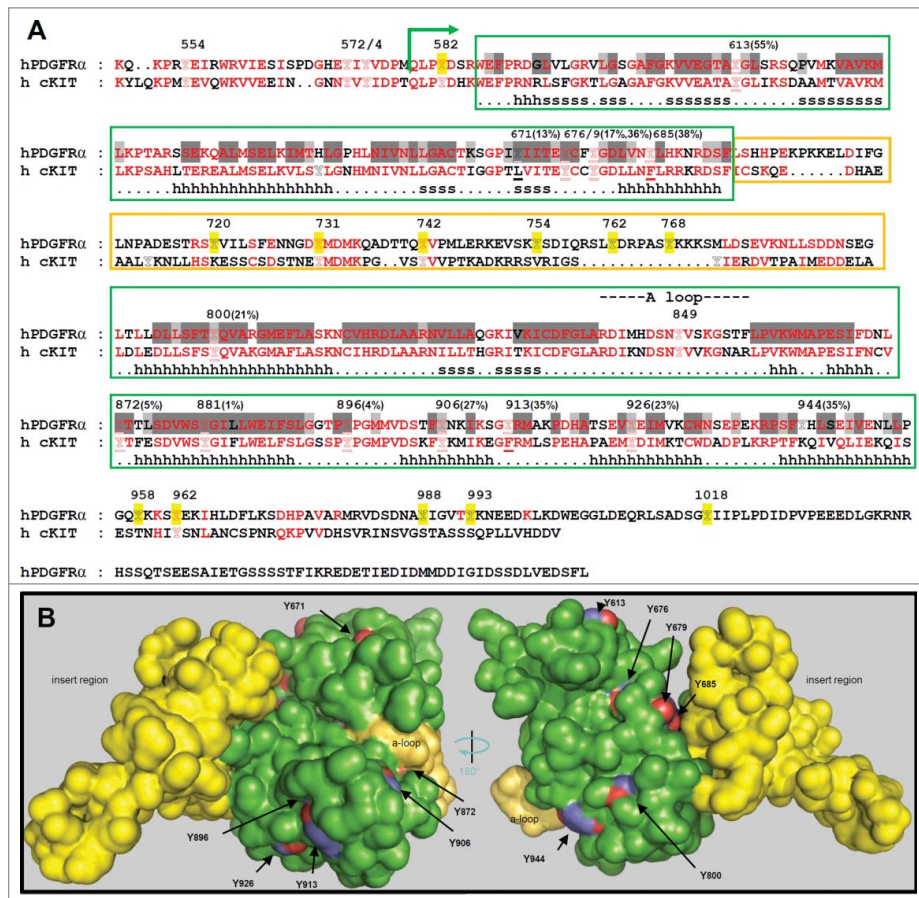
PDGFRα kinase domain can be predicted with high confidence. By calculating the relative solvent accessibility of the tyrosine residues (and all other amino acids) within the kinase domain we evaluated their potential to be phosphorylated and to serve as docking sites for signaling molecules (**Fig. 6B**). Considering solvent accessibility and the location of the proximal

neighboring residues within the tyrosine motifs we excluded all kinase domain tyrosines as potential recruitment sites for SH2 or PTB domain containing signaling molecules. An exception is the activation loop tyrosine Y^{849} which is located in a flexible region of the kinase domain. However, this tyrosine does not match known STAT recruitment motifs and its mutation would affect the activity of the kinase domain. Based on these results we mutated all 12 tyrosine residues within the flexible juxta-membrane, kinase insert and C-terminal region (mutant F/PDGFRα-12F, **Fig. 5A**). Next we assessed the activation of STAT5 via the F/PDGFRα proteins that contain a truncated FIP1L1 or mutated PDGFRα moiety. **Figure 5D** shows that STAT5 activation cannot be abrogated by a deletion within the FIP1L1 moiety or multiple point mutations of the PDGFRα moiety. A reduction of STAT5 activation can be observed for the F/PDGFRα-12F protein, but this reduction is paralleled by a reduction in PDGFRα kinase-activity which is reflected by a decrease in F/PDGFRα-12F phosphorylation on Y^{849} within the activation loop. This shows that mutation of the 12 tyrosine residues negatively affects the activity of the kinase. The absence of a clear docking site for STAT-factors in F/PDGFRα leads us to the assumption that STAT5 activation by F/PDGFRα could occur via a SH2 domain-independent mechanism.

To test this assumption (and due to the fact that we cannot definitely exclude Y^{849} in the activation loop as potential recruitment site) we decided to knock out the SH2 domain of STAT5. We thus introduced a $R^{618}Q$ mutation within the STAT5 SH2 domain to abrogate the recognition of phosphotyrosine residues by STAT5. We then stably transfected 293FR-cells ("parental cells", **Fig. 5E**, lanes 5–8) or 293FR-F/PDGFRα-cells (**Fig. 5E**, lanes 1–4) either with STAT5-wt-GFP or STAT5-R^{618}Q-GFP. As a control STAT5 phosphorylation in 293FR-cells was induced by stimulation with the cytokine OSM. **Figure 5E** shows that the functional knock-out of the STAT5 SH2 domain does not abrogate STAT5 phosphorylation via the F/PDGFRα. In contrast, OSM-induced STAT5 activation is dependent on an

intact SH2 domain. Taken together, our results show that the activation of STAT5 by F/PDGFRα does not require SH2-mediated recruitment to phosphotyrosine motifs of F/PDGFRα.

Comparison of Wild Type PDGFRα and F/PDGFRα Proteins Reveals Differences in Their Biological Responses

To investigate to what extent the observed differences in the signaling patterns for PDGFRα-wt and F/PDGFRα translate to down-stream transcriptional responses, we compared their gene expression profiles using DNA microarray analysis. Most existing methods for comparing gene-expression-data-sets require setting arbitrary cut-offs (e.g., fold changes or statistical significance), which could introduce a bias in gene filtering because of batch effect.[37,38] We therefore performed a rank-rank hypergeometric overlap (RRHO) analysis which does not require the setting of cut-offs in order to compare the transcriptomic data for PDGFRα-wt and F/PDGFRα. The RRHO method is appropriate to evaluate the similarity between gene expression profiles and discerns even weak overlap signals.[39] It identifies the statistically significant overlap while stepping through 2 lists of genes which have been ranked by their differential expression. The significance of the overlap of the 2 lists above the sliding rank threshold is represented as a RRHO heat map (**Fig. 7A**, left panel). Additionally, the data can be represented as a rank-rank scatter plot (RRSP, **Fig. 7A**, right panel). High correlation throughout the lists translates into a clustering of positive signal along the diagonal both in the RRHO heat map and scatter plot. An example for a perfect overlap (using 2 identical lists as input) is represented in **Figure 7B** and additional details on the RRHO analysis are provided in the materials and methods section. The RRHO analysis shows that the signatures of the stimulated PDGFRα-wt and the constitutively active F/PDGFRα strongly differ (**Fig. 7A**). The degree of similarity in the gene expression profiles of PDGFRα and F/PDGFRα translates into a

FIGURE 7. PDGFRα-wt and F/PDGFRα display divergent biologic responses. (**A**) Left panel: RRHO heat map comparing the transcriptomic signatures of stimulated PDGFRα-wt (14 h PDGF-AA) and F/PDGFRα. The representation is based on our microarray experiments and does not apply any cut-offs as the entire gene sets are used in the analysis. For both lists, the genes were ranked according to the ANOVA p-values attributed to the differentially expressed genes (using non-stimulated PDGFRα-wt as control). The top differentially expressed genes of both lists are located at the lower left corner of the graph. For the heat maps, the range of -log$_{10}$-transformed hypergeometric P-values are indicated in the color scale bar. High intensity signals (red) indicate the highest overlap in the lists above the current sliding rank threshold. Right panel: Rank-Rank scatter plot for the comparison of the stimulated PDGFRα-wt (14 h PDGF-AA) and F/PDGFRα transcriptomic signatures. (**B**) Rank-Rank Hypergeometric Overlap (RRHO) heat map and Rank-Rank Scatter plot for a perfect correlation (perfect overlap). The RHHO analysis was performed using 2 *identical ranked lists*.
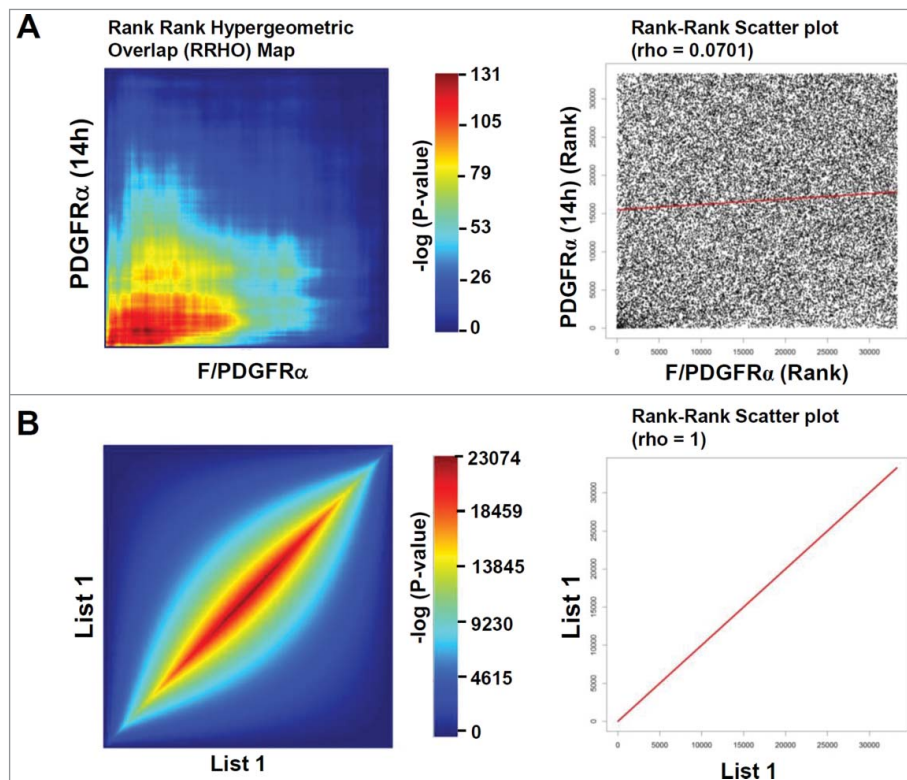
limited clustering of high ranking up-regulated genes along the diagonal axis of the heat map. **Figure 7A** also represents the corresponding rank-rank scatter plot (RRSP), where each gene is plotted by its rank and is represented as an individual dot. The representation shows a quite random pattern of distribution with only a faint increase in density in the lower left corner (representing the highest ranks in the gene list) and only a small number of genes following the diagonal. This highlights that the RRHO heat map can more efficiently monitor existing similarities between the 2 gene expression profiles than the RRSP. The gene expression profiles only contain a small number of common high ranking genes and support our observation that the signaling patterns for both proteins are strongly divergent (**Figs. 1A, 2C and 3A**).

To investigate how the activation of signaling components is linked to the transcriptomic response, we investigated the connectivity between the activated signaling components and the gene expression profiles by generating a merged signaling/transcriptomic regulatory

FIGURE 8. Common and divergent biologic responses initiated by F/PDGFRα and wild type PDGFRα. Circos plot[40] representing the generated signaling/transcriptomic regulatory networks (see materials and methods section for details on the network generation). The figure shows an overlay of the F/PDGFRα gene regulatory network and the stimulated PDGFRα-wt regulatory network. The transcriptomic signatures represent the data of the microarray analyses. Only SDEGs with a step-up FDR smaller than 0.05 and absolute fold change exceeding 40% (in comparison to non-stimulated PDGFRα-wt control cells) are represented. The SDEGs were divided into 3 groups: 1) the common regulated genes between the oncogenic situation and the PDGF-AA stimulated wild type receptor (highlighted in light green), 2) SDEGs which are only regulated in the oncogenic setting (red), 3) SDEGs which are only regulated for the PDGF-AA-stimulated (14h) wild type receptor (dark green). The average log2 transformed fold change between the corresponding situations and control is represented as a heat map in the 2 circles (outer heat map circle: F/PDGFRα; inner heat map circle: PDGF-AA stimulated PDGFRα-wt). The observed signaling characteristics are represented as conventional (violet) and unconventional (blue) signaling. The activation of these signaling components by F/PDGFRα or the PDGFRα-wt is indicated by green dots. The connections generated based on the MetaCore™ database between the molecules in the networks were visualized as violet (conventional signaling to transcriptomic responses), blue (unconventional signaling to transcriptomic responses) or gray (transcriptomic to transcriptomic) connections.
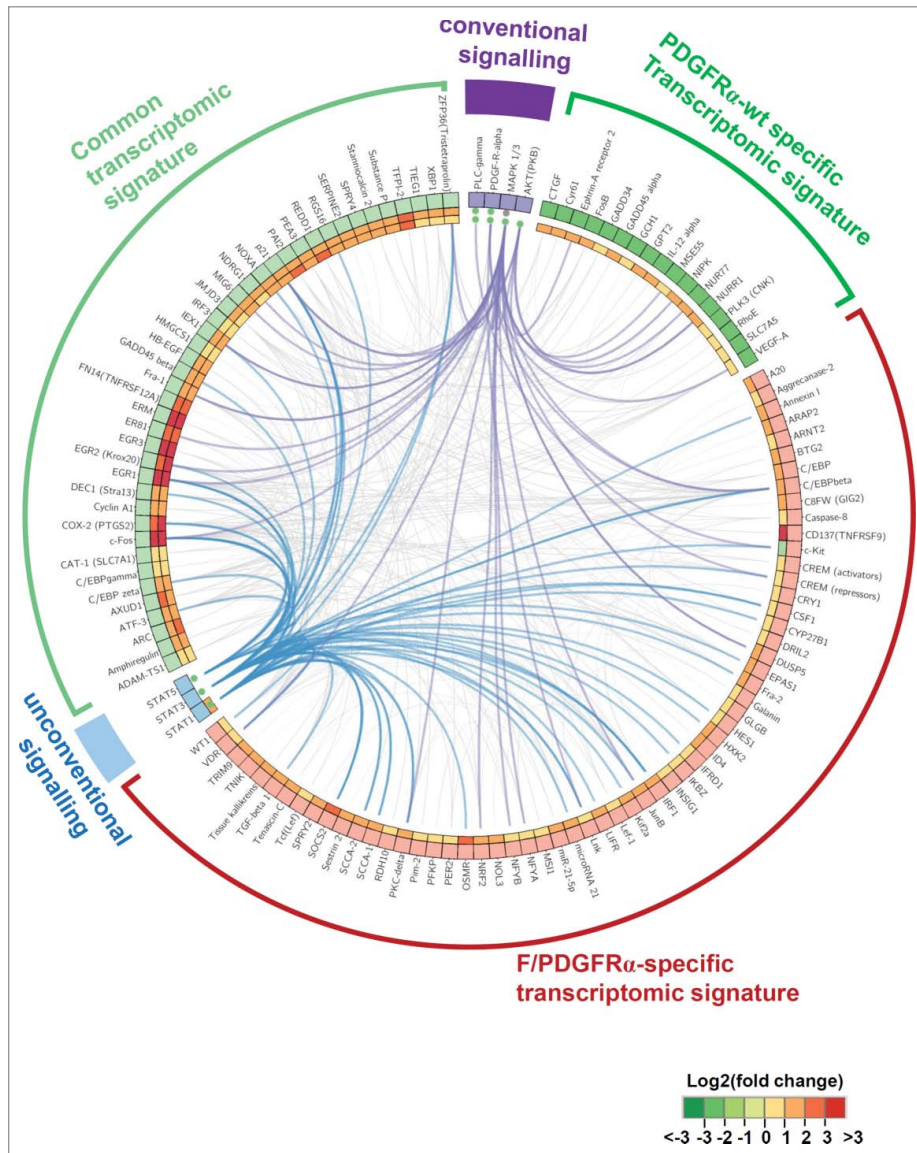
network using the MetaCore® platform (details are provided in the Materials and Methods section). We generated both a F/PDGFRα network and a PDGFRα-wt network. An overlay of both networks is represented as a Circos plot[40] in **Figure 8**. The plot integrates the data on activated signaling molecules (Western blot data, conventional (violet) and unconventional (blue) signaling) with expressed target genes (microarray data, transcriptomic signatures highlighted in green and red). As such, we aimed at analyzing the possible connectivity between the transcriptional responses (common, F/PDGFRα-specific and PDGFRα-wt-specific) and the conventional signal transduction (pPDGFRα; pPLCγ; pERK1/2 (MAPK1/3), pAKT) or the oncogene-specific unconventional signaling (pSTAT1, 3 and 5). The Circos plot illustrates that the activation of STAT factors is strongly linked to the observed oncogenic response (blue lines), highlighting the potential importance of STAT activation in the context of the F/PDGFRα transcriptomic network. Known target genes downstream of STAT factors such as SOCS2, IRF1, JunB, CEBPbeta, OSMR are part of the transcriptomic response of F/PDGFRα.

In order to further assess the importance of STAT factors for the transcriptomic response, we generated a minimal essential network highlighting the 10 functionally most relevant players in the F/PDGFRα network (details are provided in the material and methods section). **Figure 9** illustrates that STAT1 and STAT5 are identified as being among the 10 most important players (colored nodes) in the oncogenic network. These results show that STAT factor activation and responses are a central part of the F/PDGFRα mediated oncogene-specific signaling.

DISCUSSION

We aimed at analyzing the oncogenic F/PDGFRα signaling network in order to identify alternative therapeutic targets that could be useful in refractory cases of FIP1L1-PDGFRα-positive HES/CEL. Regrettably, biochemical data on F/PDGFRα is scarce and conflicting.

The primary description of F/PDGFRα reported that STAT5, but not ERK was activated by F/PDGFRα when expressed in haematopoietic cell lines such as Ba/F3.[1] A later study identified STAT5/ERK/JNK as activated signaling components downstream of the F/PDGFRα, in contrast to p38 MAPK and AKT that were found to be activated by other, unknown mechanisms.[34] Opposing data from another group identified p38 MAPK and AKT to be activated when the F/PDGFRα was retrovirally transduced.[41]

With regard to these conflicting results, we decided to perform a comparative analysis of F/PDGFRα and PDGFRα-wt under more standardized conditions, including the effects of the membrane re-localization of F/PDGFRα on its signaling behavior. We previously showed that the signaling characteristics of the wild-type PDGFRα in 293FR cells match those observed in primary fibroblasts which naturally express the PDGFRα.[20]

When comparing F/PDGFRα with PDGFRα-wt in our cellular system, we observed that F/PDGFRα rather activates STAT factor signaling than conventional PDGFRα signaling pathways. Importantly, the extent of STAT factor activation is comparable to cytokine-induced activation (**Fig. 4A**). The comparison with the oncogenic mutants (e.g., PDGFRα-D[842]V) occurring in GIST shows that pronounced STAT factor activation is a more general characteristic of oncogenic PDGFRα signaling (**Fig. 3A**).[20]

We hypothesized that the altered localization of the FIP1L1-PDGFRα fusion protein in contrast to the PDGFRα-wt could affect the signaling capacity of F/PDGFRα. Choudhary et al. demonstrated that Flt3 signaling depends on the cellular localization of the constitutively active mutants when investigating the intracellularly retained Flt3-ITD mutant protein.[42] By engineering a membrane-targeted MEM-F/PDGFRα mutant we show for the first time that notably AKT activation requires membrane localization of F/PDGFRα and that the cytoplasmic localization of F/PDGFRα does not allow this fusion protein to fully exploit its signaling capacity. Our data indicate that the reported AKT-activation in F/PDGFRα-

FIGURE 9. STAT5, STAT1 and ERK1/2 (MAPK1/3) rank among the top 10 nodes of the oncogenic gene regulatory network. Representation of the minimal essential network based on the merged signaling/transcriptomic regulatory network of F/PDGFRα (see materials and methods section for details on the minimal essential network generation). Only the 10 top nodes are highlighted by a color code and the essentiality of the nodes increases from yellow color to red color. The first neighbors of the MEN members are represented as white nodes.
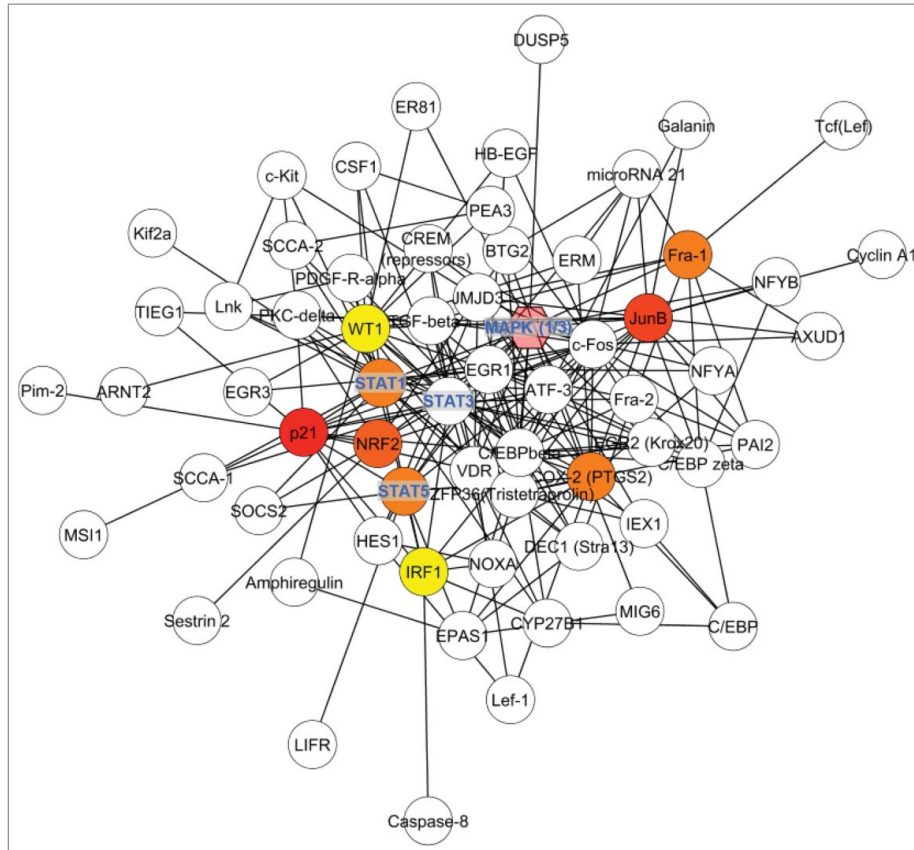
positive cells is dependent on additional triggers such as secondary mutations or additional stimuli. Also MAPK activation was clearly increased when F/PDGFRα was targeted to membranes. Moreover, we observed that the activation levels of ERK1/2 are very variable in F/PDGFRα positive cells and are often below the levels activated via PDGFRα-wild type. A possible explanation for this could be that dephosphorylation of ERK1/2 occurs 5-fold faster in the cytosol than at the plasma membrane.[43] Regardless of their activation levels, our data indicate that the observed ERK1/2 (MAPK1/3) signals translate into corresponding gene expression (e.g. expression of early growth response factors such as EGR-1 or the nuclear phosphatase DUSP5 which have been shown to be regulated upon ERK1/2 activation[44,45] (**Fig. 8**).

In spite of similar mRNA levels, we observed a higher protein expression for F/PDGFRα when compared to wild type PDGFRα. Therefore, one could argue that the different signaling capacities that we observe may be due to these differences in protein expression. However, our membrane-targeted MEM-F/PDGFRα mutant is expressed at similar levels as PDGFRα-wt and clearly shows an increase in ERK, AKT and p38 activation, strongly suggesting that the differences in

AKT, ERK and p38 activation are due to the localization and not to the protein expression levels. In addition, signaling initiated by F/PDGFRα is identical to signaling induced by the membrane-anchored PDGFRα-D842V mutant (with comparable expression levels; **Fig. 2C**). Concerning the strong difference in STAT activation, we doubt that it could be due to the different protein expression levels in our system. Our comparison of PDGFRα and OSM induced STAT activation (**Fig. 3B** and previously published work)[20] shows that PDGFRα is a very poor activator of STATs. We have obtained similar data for PDGFRβ in various cells (data not shown). The poor activation of STAT5 (in comparison to cytokine-induced signals) by wild-type PDGFRs has also recently been shown by Velghe et al., who also compared it to STAT5 activation initiated via mutant PDGFRα proteins.[46] We thus think that the cell type also does not play a major role for the observed differences in signaling. In fact, using haematopoietic cells, Choudhary et al. have shown that the activation of STAT5 by an ER-retained mutant of the closely related Flt3 receptor occurs from the intracellular compartment whereas conventional signaling (such as AKT and ERK activation) is initiated at the plasma membrane.[42] These findings are absolutely in line with our data on GIST-associated PDGFRα mutants in 293 cells.[20] Similar intracellular retention and corroborating STAT5 activation was also observed for oncogenic KIT mutants.[47] Here, we show the same localization-dependent skewed signaling behavior for F/PDGFRα. Together, all these data show that increased intracellular localization shifts the signaling capacities of the PDGFR/KIT/Flt3 family of receptors in a variety of cell types.

The importance of aberrant and constitutive activation of STAT factors in cancer is well documented.[48,49] Constitutive activation of STAT5 is known to be important for myeloid transformation.[31-33] Besides the direct effects (e.g., growth promoting or inhibiting) that STATs can exert on the tumor cell itself, they are also known to have profound effects on the tumor microenvironment.[48-50] In this context, STAT1 rather acts as a tumor suppressor whereas STAT3 is thought to be pro-oncogenic.[49] This oncogenic activity of STAT3 often occurs via the tumor microenvironment where it induces tumor-associated inflammation. The balance between STAT1 and STAT3 activation is paramount for the resulting effects on the tumor cell itself and the microenvironment.[49] The presence of activated STAT1/STAT1 homodimers is a prerequisite for an efficient STAT1 response.[51] Furthermore, the formation of STAT1/STAT1 homodimers can be influenced by the presence of activated STAT3 because of the competing formation of STAT1/STAT3 heterodimers.[51,52] The fine-tuning of STAT1 and STAT3 levels can thus have important effects on their biologic responses. Here, we describe that the oncogenic F/PDGFRα mutant protein induces the formation of STAT1/STAT1 homodimers, which then leads to the transcription of STAT1 specific target genes such as IRF1 (**Fig. 8**). However, we found most of the activated STAT3 to be present in STAT1/STAT3 heterodimers. The role of this STAT species and its potency to induce STAT3-dependent genes is not entirely clear. In our view, the formation of the STAT1 and STAT3 homo- and heterodimers is a crucial parameter which needs to be considered when investigating the biological role of F/PDGFRα mediated STAT activation. We think that the patient-specific background (and especially STAT1 and STAT3 levels and the extent of their phosphorylation) are decisive for the biologic response. In a patient-dependent manner, the response may thus shift toward a predominant activation of one of these 2 STATs, which could in turn either drive or impair tumor development and differentially affect the tumor microenvironment.

We identified STATs as central players in the F/PDGFRα specific signaling network. Patients harboring the F/PDGFRα-mutant could thus benefit from inhibition of STAT activity. The simplest approach for STAT-inhibition is targeting the upstream kinase. Other strategies would be the use of oligonucleotide (ODN) decoys as specific STAT-DNA-binding inhibitors or small molecule inhibitors that target pTyr-SH2 domain interactions.[53] In order to assess the potential targeting of STAT

activation via F/PDGFRα, we analyzed the STAT activation mechanism in more detail. Our experiments clearly indicate that STAT activation by F/PDGFRα differs from the canonical JAK/STAT-activation processes, since STAT activation is not affected by pharmacological inhibition using *next generation* Jak-inhibitors. Our results are in strong contrast to a study in which Jak2 has been proposed as upstream kinase for STAT factors in F/PDGFRα-positive cells using the inhibitor AG490.[27] However, this inhibitor is prone to generate off-target effects as it is usually used at concentrations which exceed the limits at which TKIs are assumed to generate specific effects.[54] The AG490 concentrations used by Li et al. (10–100 μM)[27] are almost 2 orders of magnitudes higher than those used for the new generation of potent JAK inhibitors (e.g. INCB018424, IC50 for Jak family members: 2.7–322 nM) that we used in our experiments. AG490 generally tends to induce dose-dependent reduction of proliferation and induction of apoptosis, in concentrations where STAT activation was not prevented.[55] Moreover, recent studies have also highlighted the low potency of AG490 for inhibition of Jak2[56] or even the total lack of Jak2-inhibition[57] at concentrations of 5 μM. Our data indicate that Jaks are no suitable drug targets in F/PDGFRα-positive cells and that it is questionable whether patients would benefit from treatment with Jak inhibitors. In several contexts oncogenic STAT activation has also been reported to involve the kinases of the Src family.[30] However, our results show that Src kinases are also not required for STAT activation via mutated PDGFRα proteins such as F/PDGFRα and PDGFRα-D[842]V.

In context of the highly homologous PDGFRβ, a phosphotyrosine-dependent recruitment of STAT5 has been reported.[10] Importantly, the corresponding tyrosine motif of PDGFRα is absent in the F/PDGFRα fusion protein. This motif also serves as recruitment and activation site for the Src kinase. Our mutational analysis of F/PDGFRα and STAT5 strongly suggests that activation of STAT5 does not require tyrosine motifs of F/PDGFRα nor a functional STAT5 SH2-domain. It should

be noted that Y849 which is required for enzymatic activity was not subjected to mutation. This finding supports the conclusion that STAT5 may directly be activated by F/PDGFRα without prior recruitment to phosphotyrosine motifs. Of course, we cannot definitely exclude that additional kinases downstream of F/PDGFRα contribute to the activation of STAT factors. Such an "auxiliary" kinase would have to be recruited via a tyrosine-independent mechanism as mutation of all accessible recruitment sites still allows STAT activation whereas all other tested signaling pathways are abrogated (data not shown). Although the SH2 domain does not contribute to the recruitment of STAT5 to the PDGFRα, it is indispensable for the dimerization of activated STAT5 and thus for its transcriptional response. As such, targeting of the SH2 domain with small molecule inhibitors is thus still a possible strategy for STAT5 inhibition in the F/PDGFRα system (especially as our results show that Jak inhibition may not be useful in this context). Small molecule inhibitors that target the SH2-domain have mostly focused on STAT3. Most recently, inhibitors that specifically target the SH2 domain of STAT5 have been developed and successfully tested for antileukemic activities in BCR-ABL and FLT3 ITD-expressing cell lines.[58] In the F/PDGFRα system, STAT5-SH2 domain inhibitors would not abrogate STAT5 phosphorylation, but impair the dimerization of phosphorylated STAT5. This implicates that direct STAT5-mediated transcriptional responses would be affected. However, targeting of the SH2 domain may not prevent dimerization-independent cytosolic functions of phosphorylated STAT5.

In brief, F/PDGFRα cannot fully exploit its capacity to activate AKT and MAPK pathways in comparison to membrane anchored PDGFRα variants (wild type or mutants). On the other hand, this "weakness" may be compensated by the shift toward STAT-mediated responses. Their activation via a non-canonical mechanism very likely also affects the sensitivity of F/PDGFRα-mediated STAT activation toward negative regulatory mechanism such as the inhibition via SOCS proteins. In our view, such

mechanisms, together with the ability of F/PDGFRα to escape ubiquitin-mediated proteasomal degradation, are crucial contributors for the oncogenic potential of F/PDGFRα. Further studies will have to dissect the contributions of these individual mechanisms and the importance of the different signaling components for the disease process. Particularly, the balance of STAT factor activation and associated anti-tumor or tumor-promoting effects will be challenging aspects which need to be addressed in the future.

MATERIALS AND METHODS

Cell Culture, Transfection, and Cytokines

Primary normal human dermal fibroblast lines (NHDF) were generously provided by Prof. Jens M. Baron (RWTH-Aachen, Germany) and their isolation was performed as described previously.[59] *Src++* (ATCC®-CRL-2497™) and *SYF* (ATCC®-CRL-2459™) MEF cells were purchased from ATCC. Transfection of the MEF cells with 0.4 μg of the respective expression plasmid (pcDNA5/FRT-FIP1L1-PDGFRα, -D842V or empty vector) was performed using the Effectene Transfection Reagent (QIAGEN; 301425) according to the manufacturer's recommendations. 293FR cells, containing FRT target site and Tet repressor (invitrogen), were maintained in DMEM supplemented with 10% fetal bovine serum (FBS, PAA Laboratories/GE Healthcare Europe GmbH) in humidified atmosphere containing 5% CO_2. EOL-1 (DMSZ: ACC 386) cells were cultivated in RPMI 1640 supplemented with 10% FBS. Cells were routinely screened for *Mycoplasma* contamination. 293FR cells were transfected using TransIT®-LT1 Transfection reagent (Mirus, MIR2300) according to the manufacturer's protocol. Stably transfected cells resulting from site directed recombination were selected and cultivated in presence of 100 μg/ml Hygromycin (Invivo-Gen; ant-hg-1) and 10 μg/ml Blasticidin (InvivoGen; ant-bl-1). Protein expression was induced under serum reduced (1%; up to 15h) followed by serum free conditions (0% FBS;

3h) with 5 ng/ml doxycycline (SigmaAldrich, D9891). Stable transfectants, constitutively expressing STAT5B-GFP or the STAT5B-GFP-SH2-mutant ($R^{618}Q$) were obtained by non-directed genomic integration and selection with 300 μg/ml G418 (InvivoGen; ant-gn-1). MG132 (Calbiochem, 474788), Janus kinase Inhibitor I (Calbiochem, 420097), INCB018424 (Seleckchem, S1378) and Imatinib/ "Gleevec" (Symansis, SY-Imatinibmesylate) were dissolved in DMSO and supplemented for the indicated times. Recombinant human OSM (working concentration: 25 ng/ml) was obtained from Peprotech (CatNo# 300-10T), recombinant human PDGFAA (working concentration: 250 ng/ml) was purchased from Immunotools (CatNo# 11343687).

Cloning and Expression Vectors

pCMV-AC-GFP-STAT5B expression construct was purchased from OriGene (CatNo. RG209429). FIP1L1-PDGFRα sequence was extracted from EOL-1 cells. Cellular RNA was isolated using the RNeasy Mini Kit (QIAGEN, 74104) and cDNA was prepared using 1st Strand cDNA Synthesis Kit for RT-PCR (Roche Applied Science, 11483188001). F/PDGFRα was amplified from cDNA and cloned into a modified pcDNA5/FRT/TO vector (Invitrogen™, V6520–20) using standard cloning procedures. The membrane targeting sequence (MEM-tag) was generated by inserting an oligonucleotide coding for the posttranslational palmitoylation sequence of neuromodulin GAP43 (MLCCMRRTKQVE-KPSG), for N-terminal expression with the fusion protein. Various Y to F-point mutations were introduced into F/PDGFRα as well as PDGFRα ($D^{842}V$) and STAT5 ($R^{618}Q$) using the QuikChange® Site-Directed Mutagenesis Kit (Stratagene/Agilent Technologies, CatNo. 200518). Mutagenesis oligonucleotides were designed using the QuikChange Primer Design tool (Agilent technologies). (1–29)-F/PDGFRα deletion mutant was generated by consecutive PCR cycles, fusing the sequence of amino acids 1–29 of FIP1L1 gene to identical PDGFRα segment (Q)[579] as in the F/PDGFRα fusion. Sequence identity was confirmed by sequencing.

Antibodies and Western Blot

Primary antibodies against PLCγ (#5690) and phosphospecific antibodies against STAT1 (Tyr[701] #9171), STAT3 (Tyr, [705] #9145), pERK1,2 (Thr[202]/Tyr [204] #9106), PDGFRα-Tyr[849]/β-Tyr,[857] #3170), AKT (Ser,[473] #9271) were purchased from Cell Signaling; anti-STAT1 (CatNo. 610116) and anti-STAT3 (CatNo. 610189) and phosphospecific antibody for STAT5 (Tyr[694], CatNo 611964) were purchase from BD; phosphospecific antibody for PLCγ1 (Tyr,[783] ProductNo 07-509) was obtained from EMD Millipore and antibodies against STAT5 (C-17: sc-835), PDGFRα (C-20: sc-338), ERK1 (K-23: sc-94), AKT1,2 (N-19: sc-1619) and tubulin (DM1A: sc-32293) were purchased from Santa Cruz Biotechnology. STAT5 antibody (C-17) was used for super-shift (EMSA). HA-antibody (6E2, Cell Signaling #2367) was used for detection of HA-tag. For Western blot analysis, cells were lysed on the plates using 1$\times$ Laemmli buffer. The proteins were separated by SDS-PAGE in 10% PAA-gels, followed by semi-dry blotting onto a 0.45 μm polyvinylidene difluoride membrane (PALL, S80306). Western blot analysis was performed using indicated primary antibodies followed by incubation with horseradish peroxidase-conjugated secondary antibodies from Cell signaling (Anti-rabbit IgG/HRP: #7074 and Anti-mouse IgG/HRP: #7076) and Dako (Anti-Goat Immunglobulins/HRP: P 0449). Signals were detected using an ECL solution containing 2.5 mM Luminol (SigmaAldrich: 123072), 2.6 mM hydrogenperoxide (SigmaAldrich: H1009), 100mM Tris-HCL/ pH8.8 (SigmaAldrich: T-1503) and 0.2 mM para-coumaric acid (SigmaAldrich: C9008).[60] Prior to reprobing, the blots were stripped in 2%SDS (Carl Roth: CN30.3), 100 mM β-mercaptoethanol (Carl Roth: 4227.3) in 62.5 mM Tris-HCl (pH6.7/ for 30 min at 70°C).

Confocal Live Cell Microscopy

HEK Flp-In-293 cells expressing MEM-GFP or GFP were seeded onto poly-L-Lysine (SigmaAldrich: P-4832), coated cover slips at least 24 h before induction with doxycycline. Induction of protein expression with doxycycline (5 ng/ml) was started 14 h prior to microscopy. Confocal live cell imaging (37°C, 5% CO2, Krebs-Ringer-Hepes medium + Glucose) was performed using a Zeiss LSM510 invert laser scanning microscope. GFP was excited with laser light of λexc = 488 nm and fluorescence was detected using a longpass filter 505 nm (LP505).

Ubiquitination

3.5×10^5 of the respective 293FR cells were transfected with 1μg of an HA-ubiquitin expression plasmid and expression of the investigated PDGFRα protein was initiated after 24 h with 5 ng/ml doxycycline. Proteasome inhibitor MG132 (10mM) was added 2 h prior to lysis and cells expressing wild-type PDGFRα were additionally stimulated with 100 ng PDGF-AA for 1 h prior to lysis. Cells were harvested 14 h after induction. Cell lysis and immunoprecipitation (using a PDGFRα-antibody from Santa Cruz Biotechnologies (C20) were performed as described previously.[61] Subsequently, the precipitated proteins were investigated by Western blot analysis.

Detergent-Free Preparation of Nuclear Extracts and Electrophoretic Mobility Shift Assay (EMSA)

Preparation of nuclear extracts and the assay was performed as previously described.[62] For binding of STAT1 and STAT3, a mutated oligonucleotide corresponding to the *sis*-inducible element of the c-*fos* promoter (m67SIE(s): 5′-GAT CCG GGA GGG ATT TAC GGG AAA TGC TG-3′; (as): 5′AAT TCA GCA TTT CCC GTA AAT CCC TCC CG-3′) was used. For STAT5 binding, an oligonucleotide corresponding to the β-casein gene promoter sequence (β-casein (s): 5′AGA TTT CTA GGA ATT CAA ATC-3′; (as) 5′GAT TTG AAT TCC AAG AAA TCT-3′) was utilized. The β-casein oligonucleotide was radioactively labeled using the 5′ end-labeling procedure.

10 μl of casein oligonucleotide (100 pmol/μl) was incubated with 5μl γ32 dATP (10 mM), 2 μl H$_2$O, 2 μl buffer A (Fermentas/Thermo Scientific: EK0031); 500mM Tris/HCl, pH7.6, 100 mM MgCl$_2$, 50 mM DTT, 1mM spermidine and 1μl T4-polynucleotide kinase (10U/μl, Fermentas/ Thermo Scientific: EK0031) for 20 min at 37°C. Protein concentrations of nuclear extracts were measured using a Nano-Drop spectrophotometer (PEQLAB/Thermo Scientific). The DNA-bound STAT complexes were visualized using a Typhoon 9410 Variable Mode Imager (Amersham Biosciences/GE Healthcare).

Molecular Modeling of the PDGFRα Kinase Domain

For molecular modeling and graphic representation of the protein structures, the programs WHAT IF[63] and Pymol [DeLano, WL (2002) The PyMOL Molecular Graphics System. DeLano Scientific, San Carlos, CA, USA] were used. The structure of the active kinase domain of cKit and a model structure of the cKit kinase insert region (Brookhaven data bank entry codes 1PKG and 1R01) were used as template for the model structure of the active PDGFRα kinase domain. The initial alignment of the intracellular sequences of human cKit and human PDGFRα was performed with BLAST.[64] Modifications were then introduced to meet structural requirements derived from the known cKit kinase domain structure. The RefSeq accession numbers for the used sequences are: NP_006197.1 (human PDGFRα) and NM_000222 (human cKIT). The relative solvent accessibility of an amino acid represents the percentage of the accessibility in the unfolded state being still available in the folded protein. The relative solvent accessibility of the amino acids in the kinase domain core structure was calculated with the WHAT IF software[63] using H$_2$O with a radius of 1.4 Å as probe.

Microarray Analysis

For all biological replicates, 3×10^6 cells were seeded 24 h prior to the start of the experiments. Cell number and viability were assessed using Cedex XS Analyzer (Innovatis, Roche Applied Sciences). Expression of PDGFRα-wt or F/PDGFRα was induced by 5 ng/ml doxycycline for a total of 14 h under serum deprived conditions (1% FBS for 11 h, 0% FBS for additional 3 h). Cells expressing the wild type PDGFRα were either stimulated with 250 ng/ml PDGF-AA for 1 h or a total of 14 h (PDGFRα-wt(1h/14 h)) or were left untreated (PDGFRα-wt(0 h)). The PDGFRα-wt (0 h) condition served as negative control for the stimulated wild type receptor and for the F/PDGFRα mutant. For microarray analysis, RNA of 3 biological replicates was isolated using the miRNeasy Mini Kit (QIAGEN, CatNo: 217004) according to manufacturer's instructions with additional on-column DNase I digestion. RNA quality and purity was assessed using a NanoDrop Spectrophotometer and a 2100 Bioanalyzer (Agilent Technologies) respectively. Only total RNA samples with no sign of degradation (RIN > 9) or contamination were used in this study. Gene Expression analysis was performed using GeneChip® Human Gene ST 1.0 arrays (Affymetrix) according to manufacturer's procedures.

The raw data in the form of Affymetrix CEL files was imported into Partek® Genomics Suite™ software (Partek GS) and the Robust Multichip Average (RMA) was applied to the data set.[65] Pre-adjustment for GC content with quantile normalization and a mean probe set summarization was used as suggested by the default pipeline of Partek GS. All arrays were thus normalized to correct for systematic difference due to sample preparation. Only the core probe sets were considered for further analysis. The generated data set was subjected to rigorous quality control detecting outliers and confounding variables. Principal Components Analysis (PCA) was applied in order to identify outliers and batch effects.[66] The differentially expressed genes (using PDGFRα-wt(0h) as control) were statistically evaluated by Partek® multi-way ANOVA, controlling for the batch effect due to scanning date. In order to control the false discovery rate (FDR), the Benjamini-Hochberg (step-up) procedure was applied.[67] Probe-sets with a step-up FDR <0.05 were

considered to be *significantly differentially expressed genes* (SDEGs). As indicated in the figure legends, most analyses were performed by additionally only considering SDEGs with an absolute fold change exceeding 40% (in comparison to non-stimulated PDGFRα-wt control cells).

Microarray data are available in the ArrayExpress database (www.ebi.ac.uk/arrayexpress) under accession number E-MTAB-2102.

Real-Time PCR

1 μg RNAs were reverse transcribed using the MultiScribe[TM] Reverse transcriptase (Cat. No.: 4311235) from Invitrogen using the manufacturer's recommendations. For quantitative RT-PCR analysis, gene expression levels were measured by the Applied Biosystems 7500 Real-Time PCR Systems using the ABsolut Blue qPCR SYBR Green ROX mix (Cat.No: AB-4323/A) from Thermo Scientific. Expression levels were determined using the qBase software (biogazelle) according to the MIQE guidelines. GeNorm was applied to find the best reference genes among 4: β actin (ActB), TATA box binding protein (TBP), Tubulin and cyclophilin A (CycloA). PDGFRα expression levels are given as normalized relative quantity (NRQ) to the reference genes. Primers used: ActB (GCACAGAGCCTCGCCTT and GTT-GTCGACGACGAGCG), TBP (ACCCAG-CAGCATCACTGTT and CGCTGGAACT-CGTCTCACTA), Tubulin (AGATCGGTGC-CAAGTTCTG and CCACCTGTGGCTT-CATTGTA), cycloA (CAGACAAGGTCC-CAAAGACA and CCATTATGGCGTGT-GAAGTC) and PDGFRa (AGTGAAGATGC-TAAAACCCACGG and AATGTTCAAA-TGTGGCCCCAGG). NRQs values were exported to the GraphPad prism software for graphic visualization and statistical analysis. Two-way ANOVA with Sidak's test for multiple comparison was used to compare the PDGFRα expression level between PDGFRα WT (n = 7), PDGFRα WT stimulated with PDGFAA for 1 hour (n = 3), for 14 hours (n = 7) and F/PDGFRα (n = 3). Statistical significance was set to 0.05.

Rank-Rank analysis

In order to compare the association and similarity of the alterations induced by F/PDGFRα and PDGFRα-wt signaling while avoiding arbitrary cut-off setting, we used the nonparametric rank-rank hypergeometric overlap analysis (RRHO)[39] to identify statistically significant overlap between these 2 gene signatures.

The probe sets were first ranked from the most significantly down-regulated to upregulated ones. Signs of –log10 transformed ANOVA p-values were set concordant to the sign of fold change between F/PDGFRα or stimulated PDGFRα-wt and control (non-stimulated wild type PDGFRα). Then, the probe sets were sorted based on these signed values. The ranked lists are provided as **Supplemental Table 1**. The results of the analysis are represented as a group of 2 plots: 1) The Rank-Rank scatter plot represents the overlap between 2 signatures. Spearman rank correlation coefficient (*rho*) was calculated between the compared 2 gene signatures.[68] 2) RRHO heat map: The heat map value represents the –log10 transformed hypergeometric p-value[69] for the likelihood of observing the observed degree of overlapped number of genes in-between the 2 rank thresholds, visualized as pixel on the map (step size was set as default). The maximum of the heat map value can be used as an indicator for the strength of the observed overlap trend between 2 ranked gene lists.[39] We used the Benjamini-Yekutieli (BY) FDR correction for multiple hypothesis correction.[70]

Network Analysis and Visualization

In order to obtain further insight into differences between F/PDGFRα and normal PDGFRα signaling we generated a merged signaling/transcriptomic gene regulatory network. Our goal was to build an integrated gene regulatory network based on differentially expressed genes and verified signaling components. The SDEGs with step-up FDR less than 0.05 and absolute fold change exceeding 40% were uploaded into MetaCore®. MetaCore® is a web-based computational platform designed

for the functional analysis of experimental data such as microarray data to identify regulatory networks and involved pathways (http://thom-sonreuters.com/metacore/). We used the most stringent direct interaction (DI) algorithms to infer the relationship between the SDEGs "seeds" with high-confidence, manually-curated, peer-reviewed and cell-type specific interactions from the MetaCore® database (non-connected clusters and genes were removed). Later manual network curation was performed with Cytoscape.[71]

From the original list of 220 coherently regulated SDEGs between F/PDGFRα and the non-stimulated PDGFRα-wt control as well as the verified activated signaling components (PDGFRα, PLCγ, ERK1/2, STAT1, STAT3 and STAT5), we obtained a global PDGFRα-mutant gene regulatory network consisting of 108 nodes and 321 function relations. Similarly, a conventional "PDGFRα-wt regulatory network" was constructed by involving only the SDEGs between PDGF-AA stimulated conditions (14h) and non–stimulated control and the active conventional signaling, which resulted in a connected graph of 61 nodes and 135 edges. An overlay of both the mutant gene regulatory network and the wild type network is shown in **Figure 8**. The list of genes is provided in **Supplemental Table 2**.

Minimal Essential Network

Identifying essential nodes/hubs is a way to decipher the critical key controllers within biochemical pathways or complex networks.[72,73] We performed network properties assessment using the Cytoscape plugin "CytoHubba" (http://www.jsbi.org/pdfs/journal1/GIW09/Poster/GIW09S003.pdf) to provide a topological analysis and allow the definition of a range of network properties which could be further used to evaluate the "essentiality" of the network nodes. The top 10 of the gene regulation network nodes ranked for their MCC (Maximal Clique Centrality) scores were used to generate a minimal essential network (MEN). The resulting MEN represents the functionally most relevant core of an Interactome model.[73]

DISCLOSURE OF POTENTIAL CONFLICTS OF INTEREST

No potential conflicts of interest were disclosed.

ACKNOWLEDGMENTS

FUNDING

SUPPLEMENTAL MATERIAL

Supplemental data for this article can be accessed on the publisher's website.

REFERENCES

1. Cools J, DeAngelo DJ, Gotlib J, Stover EH, Legare RD, Cortes J, Kutok J, Clark J, Galinsky I, Griffin JD, et al. A tyrosine kinase created by fusion of the PDGFRA and FIP1L1 genes as a therapeutic target of imatinib in idiopathic hypereosinophilic syndrome. N Engl J Med 2003; 348:1201-14; PMID:12660384; http://dx.doi.org/10.1056/NEJMoa025217

2. Griffin JH, Leung J, Bruner RJ, Caligiuri MA, Briesewitz R. Discovery of a fusion kinase in EOL-1 cells and idiopathic hypereosinophilic syndrome. Proc Natl Acad Sci U S A 2003; 100:7830-5; PMID:12808148; http://dx.doi.org/10.1073/pnas.0932698100

3. Stover EH, Chen J, Folens C, Lee BH, Mentens N, Marynen P, Williams IR, Gilliland DG, Cools J. Activation of FIP1L1-PDGFRα requires disruption of the juxtamembrane domain of PDGFRα and is FIP1L1-independent. Proc Natl Acad Sci U S A 2006; 103:8078-83; PMID:16690743

4. Bazenet CE, Gelderloos JA, Kazlauskas A. Phosphorylation of tyrosine 720 in the platelet-derived growth factor alpha receptor is required for binding of Grb2 and SHP-2 but not for activation of Ras or

cell proliferation. Mol Cell Biol 1996; 16:6926-36; PMID:8943348

5. Eriksson A, Nanberg E, Ronnstrand L, Engstrom U, Hellman U, Rupp E, Carpenter G, Heldin CH, Claesson-Welsh L. Demonstration of functionally different interactions between phospholipase C-gamma and the two types of platelet-derived growth factor receptors. J Biol Chem 1995; 270:7773-81; PMID: 7535778; http://dx.doi.org/10.1074/jbc.270.17.10161

6. Rupp E, Siegbahn A, Ronnstrand L, Wernstedt C, Claesson-Welsh L, Heldin CH. A unique autophosphorylation site in the platelet-derived growth factor alpha receptor from a heterodimeric receptor complex. Eur J Biochem 1994; 225:29-41; PMID: 7523122; http://dx.doi.org/10.1111/j.1432-1033.1994.00029.x

7. Yokote K, Hellman U, Ekman S, Saito Y, Rönnstrand L, Saito Y, Heldin CH, Mori S. Identification of Tyr-762 in the platelet-derived growth factor alpha-receptor as the binding site for Crk proteins. Oncogene 1998; 16:1229-39; PMID:9546424; http://dx.doi.org/10.1038/sj.onc.1201641

8. Hooshmand-Rad R, Yokote K, Heldin CH, Claesson-Welsh L. PDGF alpha-receptor mediated cellular responses are not dependent on Src family kinases in endothelial cells. J Cell Sci 1998; 111 (Pt 5):607-14; PMID:9454734

9. Gelderloos JA, Rosenkranz S, Bazenet C, Kazlauskas A. A Role for Src in Signal Relay by the Platelet-derived Growth Factor alpha Receptor. J Biol Chem 1998; 273:5908-15; PMID:9488729; http://dx.doi.org/10.1074/jbc.273.10.5908

10. Valgeirsdóttir S, Paukku K, Silvennoinen O, Heldin CH, Claesson-Welsh L. Activation of Stat5 by platelet-derived growth factor (PDGF) is dependent on phosphorylation sites in PDGF beta-receptor juxtamembrane and kinase insert domains. Oncogene 1998; 16:505-15; http://dx.doi.org/10.1038/sj.onc.1201555

11. Sachsenmaier C, Sadowski HB, Cooper JA. STAT activation by the PDGF receptor requires juxtamembrane phosphorylation sites but not Src tyrosine kinase activation. Oncogene 1999; 18:3583-92; PMID:10380880; http://dx.doi.org/10.1038/sj.onc.1202694

12. Yu JC, Heidaran MA, Pierce JH, Gutkind JS, Lombardi D, Ruggiero M, Aaronson SA. Tyrosine mutations within the alpha platelet-derived growth factor receptor kinase insert domain abrogate receptor-associated phosphatidylinositol-3 kinase activity without affecting mitogenic or chemotactic signal transduction. Mol Cell Biol 1991; 11:3780-5; PMID:1646396

13. Miyake S, Lupher ML, Jr., Andoniou CE, Lill NL, Ota S, Douillard P, Rao N, Band H. The Cbl protoon-cogene product: from an enigmatic oncogene to center stage of signal transduction. Crit Rev Oncog 1997; 8:189-218; PMID:9570294; http://dx.doi.org/10.1615/CritRevOncog.v8.i2-3.30

14. Fantl WJ, Escobedo JA, Williams LT. Mutations of the platelet-derived growth factor receptor that cause a loss of ligand-induced conformational change, subtle changes in kinase activity, and impaired ability to stimulate DNA synthesis. Mol Cell Biol 1989; 9:4473-8; PMID:2479827

15. Kazlauskas A, Durden DL, Cooper JA. Functions of the major tyrosine phosphorylation site of the PDGF receptor beta subunit. Cell Regul 1991; 2:413-25; PMID:1653029

16. Sjoblom T, Boureux A, Ronnstrand L, Heldin CH, Ghysdael J, Ostman A. Characterization of the chronic myelomonocytic leukemia associated TEL-PDGF beta R fusion protein. Oncogene 1999; 18:7055-62; PMID:10597306; http://dx.doi.org/10.1038/sj.onc.1203190

17. Ross TS, Gilliland DG. Transforming properties of the Huntingtin interacting protein 1/ platelet-derived growth factor beta receptor fusion protein. J Biol Chem 1999; 274:22328-36; PMID:10428802; http://dx.doi.org/10.1074/jbc.274.32.22328

18. Herren B, Rooney B, Weyer KA, Iberg N, Schmid G, Pech M. Dimerization of extracellular domains of platelet-derived growth factor receptors. A revised model of receptor-ligand interaction. J Biol Chem 1993; 268:15088-95; PMID:8325884

19. Haan S, Wuller S, Kaczor J, Rolvering C, Nocker T, Behrmann I, Haan C. SOCS-mediated downregulation of mutant Jak2 (V617F, T875N and K539L) counteracts cytokine-independent signaling. Oncogene 2009; 28:3069-80; PMID:19543316; http://dx.doi.org/10.1038/onc.2009.155

20. Bahlawane C, Eulenfeld R, Wiesinger MY, Wang J, Muller A, Girod A, Nazarov PV, Felsch K, Vallar L, Sauter T, Satagopam VP, Haan S. Constitutive activation of oncogenic PDGFRα-mutant proteins occurring in GIST patients induces receptor mislocalisation and alters PDGFRα signalling characteristics. Cell Commun Signal 2015; 13:21; PMID:25880691; http://dx.doi.org/10.1186/s12964-015-0096-8

21. Corless CL, Barnett CM, Heinrich MC. Gastrointestinal stromal tumours: origin and molecular oncology. Nat Rev 2011; 11:865-78; PMID:22089421

22. Gotlib J, Cools J, Malone JM, 3rd, Schrier SL, Gilliland DG, Coutre SE. The FIP1L1-PDGFRalpha fusion tyrosine kinase in hypereosinophilic syndrome and chronic eosinophilic leukemia: implications for diagnosis, classification, and management. Blood 2004; 103:2879-91; PMID:15070659; http://dx.doi.org/10.1182/blood-2003-06-1824

23. Toffalini F, Kallin A, Vandenberghe P, Pierre P, Michaux L, Cools J, Demoulin J-B. The fusion proteins TEL-PDGFR{beta} and FIP1L1-PDGFR{alpha} escape ubiquitination and degradation.

Haematologica 2009; 94:1085-93; PMID:19644140; http://dx.doi.org/10.3324/haematol.2008.001149

24. Demoulin JB, Essaghir A. PDGF receptor signaling networks in normal and cancer cells. Cytokine Growth Factor Rev 2014; 25:273-83; PMID: 24703957; http://dx.doi.org/10.1016/j.cytogfr.2014. 03.003

25. Fambrough D, McClure K, Kazlauskas A, Lander ES. Diverse signaling pathways activated by growth factor receptors induce broadly overlapping, rather than independent, sets of genes. Cell 1999; 97:727-41; PMID:10380925; http://dx.doi.org/10.1016/ S0092-8674(00)80785-0

26. van Roeyen CR, Ostendorf T, Denecke B, Bokemeyer D, Behrmann I, Strutz F, Lichenstein HS, LaRochelle WJ, Pena CE, Chaudhuri A, et al. Biological responses to PDGF-BB versus PDGF-DD in human mesangial cells. Kidney Int 2006; 69:1393-402; PMID:16557224

27. Li B, Zhang G, Li C, He D, Li X, Zhang C, Tang F, Deng X, Lu J, Tang Y, et al. Identification of JAK2 as a mediator of FIP1L1-PDGFRA-induced eosinophil growth and function in CEL. PLoS One 2012; 7: e34912; PMID:22523564; http://dx.doi.org/10.1371/ journal.pone.0034912

28. Paukku K, Valgeirsdóttir S, Saharinen P, Bergman M, Heldin CH, Silvennoinen O. Platelet-derived growth factor (PDGF)-induced activation of signal transducer and activator of transcription (Stat) 5 is mediated by PDGF beta-receptor and is not dependent on c-src, fyn, jak1 or jak2 kinases. Biochem J 2000; 345:759-66; PMID:10642538; http://dx.doi. org/10.1042/0264-6021:3450759

29. Turkson J, Bowman T, Garcia R, Caldenhoven E, De Groot RP, Jove R. Stat3 activation by Src induces specific gene regulation and is required for cell transformation. Mol Cell Biol 1998; 18:2545-52; PMID:9566874

30. Yu H, Jove R. The STATs of cancer–new molecular targets come of age. Nat Rev 2004; 4:97-105; PMID:14964307

31. Hoelbl A, Kovacic B, Kerenyi MA, Simma O, Warsch W, Cui Y, Beug H, Hennighausen L, Moriggl R, Sexl V. Clarifying the role of Stat5 in lymphoid development and Abelson-induced transformation. Blood 2006; 107:4898-906; PMID:16493008; http:// dx.doi.org/10.1182/blood-2005-09-3596

32. Moriggl R, Sexl V, Kenner L, Duntsch C, Stangl K, Gingras S, Hoffmeyer A, Bauer A, Piekorz R, Wang D, et al. Stat5 tetramer formation is associated with leukemogenesis. Cancer Cell 2005; 7:87-99; PMID:15652752; http://dx.doi.org/10.1016/j.ccr. 2004.12.010

33. Ye D, Wolff N, Li L, Zhang S, Ilaria RL, Jr. STAT5 signaling is required for the efficient induction and maintenance of CML in mice. Blood 2006;

107:4917-25; PMID:16522816; http://dx.doi.org/ 10.1182/blood-2005-10-4110

34. Ishihara K, Kitamura H, Hiraizumi K, Kaneko M, Takahashi A, Zee O, Seyama T, Hong J, Ohuchi K, Hirasawa N. Mechanisms for the proliferation of eosinophilic leukemia cells by FIP1L1-PDGFRα. Biochem Biophy Res Commun 2008; 366:1007-11; PMID:18086564; http://dx.doi.org/10.1016/j.bbrc. 2007.12.063

35. Mori S, Ronnstrand L, Yokote K, Engstrom A, Courtneidge SA, Claesson-Welsh L, Heldin CH. Identification of two juxtamembrane autophosphorylation sites in the PDGF beta-receptor; involvement in the interaction with Src family tyrosine kinases. Embo J 1993; 12:2257-64; PMID:7685273

36. Noel LA, Arts FA, Montano-Almendras CP, Cox L, Gielen O, Toffalini F, Marbehant CY, Cools J, Demoulin JB. The tyrosine phosphatase SHP2 is required for cell transformation by the receptor tyrosine kinase mutants FIP1L1-PDGFRalpha and PDGFRalpha D842V. Mol Oncol 2014; 8:728-40; PMID:24618081; http://dx.doi.org/10.1016/j.molonc. 2014.02.003

37. Detours V, Dumont JE, Bersini H, Maenhaut C. Integration and cross-validation of high-throughput gene expression data: comparing heterogeneous data sets. FEBS Lett 2003; 546:98-102; PMID:12829243; http://dx.doi.org/10.1016/S0014-5793(03)00522-2

38. Warnat P, Eils R, Brors B. Cross-platform analysis of cancer microarray data improves gene expression based classification of phenotypes. BMC Bioinformatics 2005; 6:265; PMID:16271137; http://dx.doi. org/10.1186/1471-2105-6-265

39. Plaisier SB, Taschereau R, Wong JA, Graeber TG. Rank-rank hypergeometric overlap: identification of statistically significant overlap between gene-expression signatures. Nucleic Acids Res 2010; 38:e169; PMID:20660011; http://dx.doi.org/10.1093/nar/ gkq636

40. Krzywinski M, Schein J, Birol I, Connors J, Gascoyne R, Horsman D, Jones SJ, Marra MA. Circos: an information aesthetic for comparative genomics. Genome Res 2009; 19:1639-45; PMID:19541911; http://dx.doi.org/10.1101/gr.092759.109

41. Buitenhuis M, Verhagen LP, Cools J, Coffer PJ. Molecular mechanisms underlying FIP1L1-PDGFRA-mediated myeloproliferation. Cancer Res 2007; 67:3759-66; PMID:17440089; http://dx.doi. org/10.1158/0008-5472.CAN-06-4183

42. Choudhary C, Olsen JV, Brandts C, Cox J, Reddy PN, Bohmer FD, Gerke V, Schmidt-Arras DE, Berdel WE, Muller-Tidow C, et al. Mislocalized activation of oncogenic RTKs switches downstream signaling outcomes. Mol Cell 2009; 36:326-39; PMID: 19854140; http://dx.doi.org/10.1016/j.molcel.2009. 09.019

43. Harding A, Tian T, Westbury E, Frische E, Hancock JF. Subcellular localization determines MAP kinase signal output. Curr Biol 2005; 15:869-73; PMID:15886107; http://dx.doi.org/10.1016/j.cub. 2005.04.020

44. Hodge C, Liao J, Stofega M, Guan K, Carter-Su C, Schwartz J. Growth hormone stimulates phosphorylation and activation of elk-1 and expression of c-fos, egr-1, and junB through activation of extracellular signal-regulated kinases 1 and 2. J Biol Chem 1998; 273:31327-36; PMID:9813041; http://dx.doi.org/ 10.1074/jbc.273.47.31327

45. Kucharska A, Rushworth LK, Staples C, Morrice NA, Keyse SM. Regulation of the inducible nuclear dual-specificity phosphatase DUSP5 by ERK MAPK. Cell Signall 2009; 21:1794-805; PMID:19666109; http://dx.doi.org/10.1016/j.cellsig.2009.07.015

46. Velghe AI, Van Cauwenberghe S, Polyansky AA, Chand D, Montano-Almendras CP, Charni S, Hallberg B, Essaghir A, Demoulin JB. PDGFRA alterations in cancer: characterization of a gain-of-function V536E transmembrane mutant as well as loss-of-function and passenger mutations. Oncogene 2014; 33:2568-76; PMID:23752188; http://dx.doi.org/ 10.1038/onc.2013.218

47. Xiang Z, Kreisel F, Cain J, Colson A, Tomasson MH. Neoplasia Driven by Mutant c-KIT Is Mediated by Intracellular, Not Plasma Membrane, Receptor Signaling. Mol Cell Biol 2007; 27:267-82; PMID:17060458; http://dx.doi.org/10.1128/MCB.01153-06

48. Yu H, Pardoll D, Jove R. STATs in cancer inflammation and immunity: a leading role for STAT3. Nat Rev 2009; 9:798-809; PMID:19851315

49. Avalle L, Pensa S, Regis G, Novelli F, Poli V. STAT1 and STAT3 in tumorigenesis: A matter of balance. JAKSTAT 2012; 1:65-72; PMID:24058752

50. Groner B, Lucks P, Borghouts C. The function of Stat3 in tumor cells and their microenvironment. Sem Cell Dev Biol 2008; 19:341-50; PMID:18621135; http://dx.doi.org/10.1016/j.semcdb.2008.06.005

51. Haan S, Keller JF, Behrmann I, Heinrich PC, Haan C. Multiple reasons for an inefficient STAT1 response upon IL-6-type cytokine stimulation. Cell Signall 2005; 17:1542-50; PMID:15935617; http://dx.doi.org/10.1016/j.cellsig.2005.03.010

52. Costa-Pereira AP, Tininini S, Strobl B, Alonzi T, Schlaak JF, Is'harc H, Gesualdo I, Newman SJ, Kerr IM, Poli V. Mutational switch of an IL-6 response to an interferon-gamma-like response. Proc Natl Acad Sci U S A 2002; 99:8043-7; PMID:12060750; http://dx.doi.org/10.1073/pnas.122236099

53. Miklossy G, Hilliard TS, Turkson J. Therapeutic modulators of STAT signalling for human diseases. Nat Rev Drug Discov 2013; 12:611-29; PMID:23903221; http://dx.doi.org/10.1038/nrd4088

54. Knight ZA, Shokat KM. Features of selective kinase inhibitors. Chem Biol 2005; 12:621-37; PMID: 15975507; http://dx.doi.org/10.1016/j.chembiol. 2005.04.011

55. Kreis S, Munz GA, Haan S, Heinrich PC, Behrmann I. Cell density dependent increase of constitutive signal transducers and activators of transcription 3 activity in melanoma cells is mediated by Janus kinases. Mol Cancer Res 2007; 5:1331-41; PMID:18171991; http://dx.doi.org/10.1158/1541-7786.MCR-07-0317

56. Hantschel O, Warsch W, Eckelhart E, Kaupe I, Grebien F, Wagner KU, Superti-Furga G, Sexl V. BCR-ABL uncouples canonical JAK2-STAT5 signaling in chronic myeloid leukemia. Nat Chem Biol 2012; 8:285-93; PMID:22286129; http://dx.doi.org/ 10.1038/nchembio.775

57. Gabler K, Rolvering C, Kaczor J, Eulenfeld R, Mendez SA, Berchem G, Palissot V, Behrmann I, Haan C. Cooperative effects of Janus and Aurora kinase inhibition by CEP701 in cells expressing Jak2V617F. J Cell Mol Med 2013; 17:265-76; PMID:23301855; http://dx.doi.org/10.1111/jcmm.12005

58. Page BD, Khoury H, Laister RC, Fletcher S, Vellozo M, Manzoli A, Yue P, Turkson J, Minden MD, Gunning PT. Small molecule STAT5-SH2 domain inhibitors exhibit potent antileukemia activity. J Med Chem 2011; 55:1047-55; http://dx.doi.org/10.1021/ jm200720n

59. Neis MM, Wendel A, Wiederholt T, Marquardt Y, Joussen S, Baron JM, Merk HF. Expression and induction of cytochrome p450 isoenzymes in human skin equivalents. Skin Pharmacol Physiol 2010; 23:29-39; PMID:20090406; http://dx.doi.org/10. 1159/000257261

60. Haan C, Behrmann I. A cost effective non-commercial ECL-solution for Western blot detections yielding strong signals and low background. J Immunol Methods 2007; 318:11-9; PMID:17141265; http://dx. doi.org/10.1016/j.jim.2006.07.027

61. Wiesinger MY, Haan S, Wüller S, Kauffmann ME, Recker T, Küster A, Heinrich PC, Müller-Newen G. Development of an IL-6 inhibitor based on the functional analysis of murine IL-6Ra. Chem Biol 2009; 16:783-94; PMID:19635415; http://dx.doi.org/ 10.1016/j.chembiol.2009.06.010

62. Haan S, Haan C. Detection of activated STAT species using electrophoretic mobility shift assay (EMSA) and potential pitfalls arising from the use of detergents. Meth Mol Biol 2013; 967:147-59

63. Vriend G. WHAT IF: a molecular modeling and drug design program. J Mol Graph 1990; 8:52-6, 29; PMID:2268628; http://dx.doi.org/10.1016/0263-7855 (90)80070-V

64. Altschul SF, Madden TL, Schaffer AA, Zhang J, Zhang Z, Miller W, Lipman DJ. Gapped BLAST and PSI-BLAST: a new generation of protein database

search programs. Nucleic Acids Res 1997; 25:3389-402; PMID:9254694; http://dx.doi.org/10.1093/nar/25.17.3389

65. Irizarry RA, Hobbs B, Collin F, Beazer-Barclay YD, Antonellis KJ, Scherf U, Speed TP. Exploration, normalization, and summaries of high density oligonucleotide array probe level data. Biostatistics 2003; 4:249-64; PMID:12925520; http://dx.doi.org/10.1093/biostatistics/4.2.249

66. Tenenbaum JB, de Silva V, Langford JC. A global geometric framework for nonlinear dimensionality reduction. Science 2000; 290:2319-23; http://dx.doi.org/10.1126/science.290.5500.2319

67. Benjamini Y, Hochberg Y. Controlling the false discovery rate: a practical and powerful approach to multiple testing. JRSSB 1995; 57:289-300

68. Myers JL, Well AD. Research Design and Statistical Analysis. Lawrence Erlbaum Associates; 2003

69. Li X, Ni LM. A pipeline architecture for computing cumulative hypergeometric distributions. IEEE 7th Symposium on Computer Arithmetic (ARITH) 1985:166-72

70. Pollard KS, Dudoit S, Laan MJVD. Applications of Multiple Testing Procedures: ALL Data. 2005:1-26

71. Shannon P, Markiel A, Ozier O, Baliga NS, Wang JT, Ramage D, Amin N, Schwikowski B, Ideker T. Cytoscape: a software environment for integrated models of biomolecular interaction networks. Genome Res 2003; 13:2498-504; http://dx.doi.org/10.1101/gr.1239303

72. Lin CY, Chin CH, Wu HH, Chen SH, Ho CW, Ko MT. Hubba: hub objects analyzer–a framework of interactome hubs identification for network biology. Nucleic Acids Res 2008; 36:W438-43; PMID:18503085; http://dx.doi.org/10.1093/nar/gkn257

73. Stevens A, Hanson D, Whatmore A, Destenaves B, Chatelain P, Clayton P. Human growth is associated with distinct patterns of gene expression in evolutionarily conserved networks. BMC Gen 2013; 14:547; PMID:23941278; http://dx.doi.org/10.1186/1471-2164-14-547